CHAPTER 1
INTRODUCTION

1.1 Preamble

Members that are slender and support loadings that are applied perpendicular to their longitudinal axis are called beams. In general beams are long straight bars having a constant cross sectional area. Often they are classified as to how they are supported .For example a simply supported beam is pinned at one end roller supported at the other. A cantilever beam is fixed at one end free at the other .An overhanging beam has one or both of its ends freely extended over its supports. Certainly beams may be considered among the most important of all structural elements. Examples include members used to support to support the floor of a building, the deck of a bridge or the wing of an aircraft. Also the axle of an automobile, the boom of a crane , even many of the bones of the body act as beams.

Because of the applied loadings, beams develop an internal shear force and bending moment that very from point to point along the axis of the beam. The classical tools of Mechanics of Materials are derived from mathematical physics and in many cases they are not sufficient to describe the stress distribution in engineering structures. They are also inadequate to give information regarding local stress near the loads and near the supports of beams. Among the great number of problems conforming this field of science, there is necessity of profound investigation of the properties of elastic materials and the construction of a mathematical theory, which would permit studying as completely as possible the internal forces occurring in an elastic body under the action of external forces as well as the deformation of a body i.e., the change of its shape. This led to the emergence of a special trend in physics, i.e. the Theory of Elasticity to apply to elastic solids [1-3]. Individual members such as beams, columns, shafts, plates, shells etc may be modeled using either of the classical or the elasticity based mathematical approach. However, each process has got some of its own advantages as well as limitations.

The equations of theory of elasticity are a system of partial differential equations. Due to the nature of the mathematics involved in solving such equations, manual solutions have been only

developed for relatively simple geometries. For complex geometries, computation using a modern computer is considered more suitable for better solution.

1.2 Literature Review

The foundation of the classical theory of elastic beam was laid down in the 18^{th} century (1705-1750) by Leonhard Paul Euler and Daniel Bernoulli. It was then Claude-Louis Navier, who gave the details of the relation between the cross-section and the bending stiffness parameter in 1819. This theory has remained as an exact solution of the equations of three-dimensional elasticity in the case of homogenous bending, i.e. for a beam with constant bending moment. Since then the elementary methods of strength of materials were the primary tools of the practicing engineers for handling the engineering problems of structural elements for long time. However these methods are often found inadequate to furnish satisfactory information regarding local stresses near the loads and near the supports of the structures. The elementary theory gives no means of investigating stresses in regions of sharp variation in cross section of beams or shafts. Stresses in screw threads, around various shapes of holes in structures, near contact points on gear teeth, rollers and balls of bearings, have all remained beyond the scope of elementary theories. It is thus obvious that, for the designers of modern machines, recourse to the more powerful methods of the Theory of Elasticity is the necessity of time.

Considerable progress could have been made in solving important practical problems of stress analysis using the methods of theory of elasticity. In cases where a rigorous solution could not be obtained, approximate methods have been developed. In other cases, where even approximate methods could not be developed, solutions have been obtained by using experimental methods. Photoelastic methods, soap-film methods, application of strain gages, moiré fringe etc. are some of these experimental methods applied in the study of stress concentration at points of sharp variation of cross-sectional dimension and at sharp fillets of re-entrant corners. These results have considerably influenced the modern design of machine parts and helped in many cases to improve the construction by eliminating weak spots through which crack may switch on and thereby propagate.

The field of elasticity deals mainly with deformation parameters and stress parameters for the solution of two dimensional problems since most of the three-dimensional problems may be resolved to a two dimensional one. If it remains beyond the extent of analytical studies anyway, the problem has to be handled experimentally as a particular case.

Although the theories of elasticity had been established long before, the solutions of practical problems started mainly after the introduction of a stress function by George Biddell Airy, a British astrologer and mathematician, in 1862 [1]. The Airy's stress function is governed by a fourth order partial deferential equation and stress components are related to it through its various second order derivatives. The stress function solutions were initially sought taking polynomial expressions of various degrees and suitably adjusting their coefficients. By this way, a number of practically important problems of long rectangular strips could be solved [2-3]. But the success of this approach was very limited. Using these polynomial expressions, an elementary derivation of the effect of the shearing force on the curvature of the deflection curve of beams were made by Rankine [4] and by Grashof [5]. The problem of stresses in masonry dams is of great practical interest and has been attempted for solution using polynomial expressions for the stress functions [6-7]. But the solutions obtained do not satisfy the conditions at the bottom of the dam where it is connected with the foundation.

Thereafter the use of trigonometric series is considered more fruitful in producing results instead of polynomial expressions. The first application of trigonometric series in the solution of elastic problems using stress function method was given by Ribiere in his thesis [8]. Further progress in the application of these solutions was made by Filon [9]. Several particular examples were worked by Bleich [10].

Then the use of Fourier series has come into being for the structural analysis. Beyer [11] solved the problem of a continuous beam on equidistant supports under gravity loading using Fourier series. Stress function technique has also been used by Ribiere [12] for analyzing the stresses around a circular hole in plate, by Flamant [13] for stresses around a concentrated load on a straight boundary and by Stokes [14] for stresses around a concentrated load on a beam. A number of works are found with the stress function in this regard [15- 18]. Even tough the stress analysis problems are bearing enumerable shortcomings to be addressed yet.

The stumbling block of obtaining exact solution using stress function is the inability of managing the physical conditions imposed on them, i.e., management of boundary conditions of practical problems. Boundary restraints specified in terms of the displacement components cannot be satisfactorily imposed on the stress function. Since most of the practical problems in elasticity are of mixed boundary conditions, the approach fails to provide any explicit understanding of the state of stresses at the critical regions of supports and loadings. Moreover, the famous Saint Venant's principle is still applied and its merit is evaluated in solving problems of solid mechanics in which full boundary effects could not be taken into account satisfactorily in the process of solution [19-21]. For complex shapes of boundary, the difficulties of obtaining analytical solutions become formidable. These difficulties were partially avoided by renovating to experimental methods, such as extensometers, strain gauges or photoelastic methods. Using Photoelasticity, Hetengi investigated the stresses in the threads of a bolt and nut fastening. Most of the experimental investigations of elastic problems are reported in the "handbook of Experimental Stress Analysis" [22] and in "Photoelasticity" by Frocht [23]. Even now, photoelastic studies are being carried out for classical problems like uniformly loaded beams on two supports mainly because the boundary effects could not be taken into account fully in the analytical method of solutions.

The drawback of Airy's stress function and the difficulties of experimental works led to works for finding ways to solve the engineering problems where boundary conditions are set in terms of displacements. Thus the displacement formulation was introduced for those problems where boundary restraints exist [24]. This process involves finding of two displacement functions simultaneously from the two second-order elliptic partial differential equations of equilibrium, which is extremely difficult and the problem becomes more serious when the boundary conditions are mixed. The difficulties involved in trying to solve practical stress problems using the existing models have been pointed out by Durelli and Ranganayakamma [25]. The complications for solution beams especially short/deep beams were also brought to light by Rehfield and Murthy [26], Murty [27], Suzuki [28], and Hardy [29].

Since neither the stress function nor the displacement formulation is suitable for solving problems of mixed-boundary conditions, a new mathematical model called displacement

potential formulation is used to solve the elastic problems [30-37]. The current modelling approach reduces the two dimensional problem to the solution of a single differential equations of equilibrium and also enables the mixed mode of the boundary conditions to be managed appropriately. It is worth mentioning that a number of researchers worked on the advancement of displacement potential approach to handle the beam and column like structures with different loading and supporting conditions. Ahmed et. al. have developed numerical solution of both ends fixed deep beams based on displacement potential formulation [30]. Ahmed et. al. [31] have carried out investigation of stresses at the fixed end of deep cantilever beams. Akanda et. al. have carried out stress analysis of gear teeth using displacement potential function and finite differences [32]. The potential of the formulation has also been investigated by Ahmed et. al. [33] to design optimum shapes of tire-treads for avoiding lateral slippage between tires and roads. Recently, Ahmed et. al. [34] have proposed a general mathematical formulation for finite-difference solution of mixed-boundary-value problems of anisotropic materials. Further, Debnath et. al. have carried out analytical solution of short stiffened flat composite bars under axial loadings [35], and stiffened orthotropic composite panels under uniaxial tensile load [37]. All these solutions are mainly applicable for rigid boundaries; none of them is applicable to a guided beam under bending. As such the solution for guided structural element is yet to be developed.

1.3 Objectives

The present study is an attempt to extend the capability of the displacement potential formulation order to address the structural analysis of guided simply supported beams having mixed boundary conditions. The main objectives of the present research work are summarized as follows:

1. To develop a suitable scheme for obtaining analytical solution of the plane elastic field of a guided simply supported beam.
2. To analyze the deformed shape as well as the distribution of different displacement and stress components of interest in the perspective of beam depth and span.
3. To investigate the effect of different aspect ratio.

CHAPTER 2
MATHEMATICAL FORMULATION

2.1 Problem Articulation

A rectangular section simply supported beam of length L, width D and thickness W (considered to be unity for plane stress condition) is subjected to a point loading at the mid-span its top boundary and simply supporting at its bottom two corners. By this symmetric loading arrangement the beam is in equilibrium as shown in figure 2.1. Both lateral edges of the beam i.e. at x=0 and x=L are roller guided so that the axial displacements are restrained, but the lateral displacements are allowed to have any value.

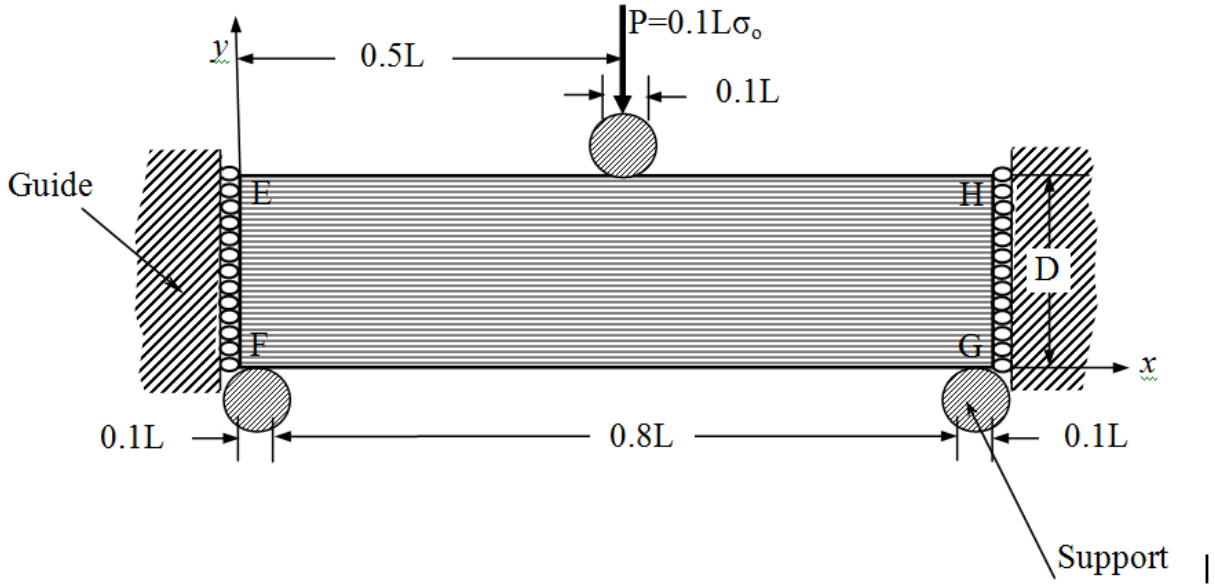

Fig. 2.1 Geometry and loading (symmetric) of the guided simply supported beam under three point bending

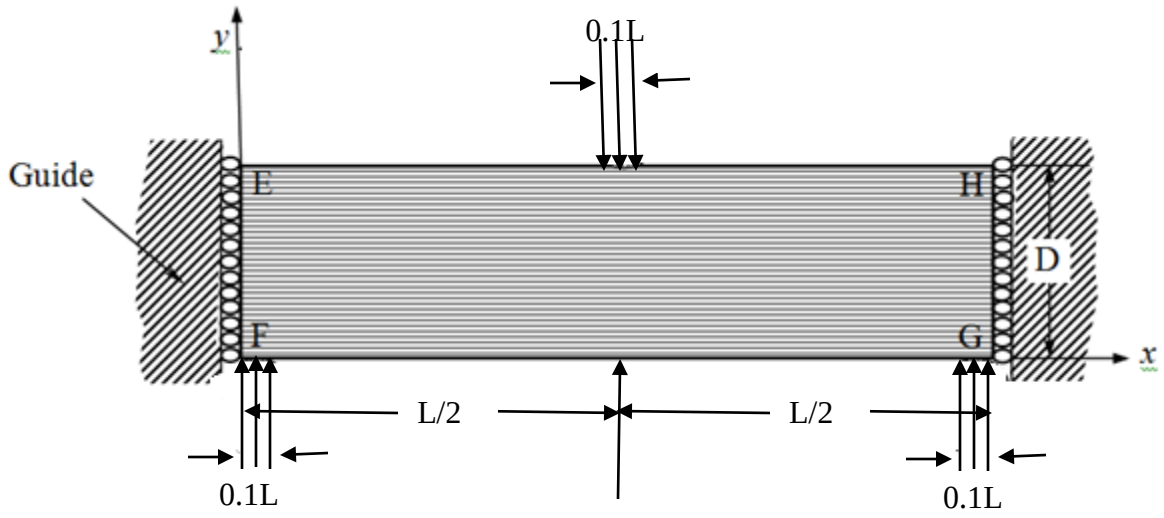

Fig 2.2 Analytical model of the guided simply supported beam

2.2 Boundary Conditions

The physical conditions at different boundaries of the beam are expressed mathematically as follows:

(i) $u_x = 0$ at the edge of $x = 0$

(ii) $u_x = 0$ at the edge of $x = L$

(iii) $\sigma_{xy}(0, y) = 0$ at the edge of $x = 0$

(iv) $\sigma_{xy}(L, y) = 0$ at the edge of $x = L$

(v) $\sigma_{xy}(x, 0) = 0$ at the edge of $y = 0$

(vi) $\sigma_{xy}(x, D) = 0$ at the edge of $y = D$

(vii) The lateral stress at the edge of $y = D$ is related to the applied load for the three point bending. Since the point load is actually acting over a certain area of the beam, for instance it can be considered for the length of x=0.45L to 0.55L. Again it is considered that the load intensity is σ_o. Therefore, the magnitude of point load, P= $0.1L\sigma_o$. Then $\sigma_{yy}(x, D) = \sigma_0$ for x=0.45L to 0.55L

(viii) Similarly, the lateral stress at the edge of $y = 0$ is related to the reactions at the support. In this case $\sigma_{yy}(x,0) = \sigma_0 / 2$ for x=0 to 0.1L and 0.9L to L.

2.3 Analytical Solution

The equation of equilibrium for isotropic material is as follows:

$$\frac{\partial^4 \psi}{\partial x^4} + 2\frac{\partial^4 \psi}{\partial x^2 \partial y^2} + \frac{\partial^4 \psi}{\partial y^4} = 0 \tag{2.1}$$

The expressions of displacement and stress components in terms of function $\psi(x, y)$ are as follows:

$$u_x(x,y) = \frac{\partial^2 \psi}{\partial x \partial y} \tag{2.2a}$$

$$u_y(x,y) = -\frac{1}{1+\mu}\left[2\frac{\partial^2 \psi}{\partial x^2} + (1-\mu)\frac{\partial^2 \psi}{\partial y^2}\right] \tag{2.2b}$$

$$\sigma_{xx}(x,y) = -\frac{E}{(1+\mu)^2}\left[\frac{\partial^3 \psi}{\partial x^2 \partial y} - \mu\frac{\partial^2 \psi}{\partial y^2}\right] \tag{2.2c}$$

$$\sigma_{yy}(x,y) = -\frac{E}{(1+\mu)^2}\left[(2+\mu)\frac{\partial^3 \psi}{\partial x^2 \partial y} + \frac{\partial^3 \psi}{\partial y^3}\right] \tag{2.2d}$$

$$\sigma_{xy}(x,y) = -\frac{E}{(1+\mu)^2}\left[\frac{\partial^3 \psi}{\partial x^3} - \mu\frac{\partial^3 \psi}{\partial x \partial y^2}\right] \tag{2.2e}$$

The potential function $\psi(x, y)$ is first assumed in a way so that the physical conditions of the two opposing guided ends are automatically satisfied. At the same time solution has to satisfy the 4th order bi-harmonic partial differential governing equation. After a long trial and error process, the solution of the governing equation (2.1) is thus approximated as follows, which gives the result:

$$\psi(x, y) = \sum_{m=1}^{\infty} Y_m(y)\cos\alpha x + K\, y^3 \tag{2.3}$$

where, $Y_m = f(y)$, $\alpha = (m\pi / L)$, K is an arbitrary constant and m = 1, 2, 3, …….∞.

Derivatives of equation (2.3) with respect to x and y are

$$\frac{\partial \psi}{\partial x} = -\sum_{m=1}^{\infty} Y_m \alpha \sin \alpha x$$

$$\frac{\partial^2 \psi}{\partial x^2} = -\sum_{m=1}^{\infty} Y_m \alpha^2 \cos \alpha x$$

$$\frac{\partial^3 \psi}{\partial x^3} = \sum_{m=1}^{\infty} Y_m \alpha^3 \sin \alpha x$$

$$\frac{\partial^4 \psi}{\partial x^4} = \sum_{m=1}^{\infty} Y_m \alpha^4 \cos \alpha x$$

$$\frac{\partial^2 \psi}{\partial x \partial y} = -\sum_{m=1}^{\infty} Y_m' \alpha \sin \alpha x$$

$$\frac{\partial^3 \psi}{\partial x \partial y^2} = -\sum_{m=1}^{\infty} Y_m'' \alpha \sin \alpha x$$

$$\frac{\partial^3 \psi}{\partial x^2 \partial y} = -\sum_{m=1}^{\infty} Y_m' \alpha^2 \cos \alpha x$$

$$\frac{\partial^4 \psi}{\partial x^2 \partial y^2} = -\sum_{m=1}^{\infty} Y_m'' \alpha^2 \cos \alpha x$$

$$\frac{\partial \psi}{\partial y} = \sum_{m=1}^{\infty} Y_m' \cos \alpha x + 3Ky^2$$

$$\frac{\partial^2 \psi}{\partial y^2} = \sum_{m=1}^{\infty} Y_m'' \cos \alpha x + 6Ky$$

$$\frac{\partial^3 \psi}{\partial y^3} = \sum_{m=1}^{\infty} Y_m''' \cos \alpha x + 6K$$

$$\frac{\partial^4 \psi}{\partial y^4} = \sum_{m=1}^{\infty} Y_m'''' \cos \alpha x$$

Substituting the expressions of above derivatives in Eq. (3.1) following equation is obtained.

$$\sum_{m=1}^{\infty} Y_m \alpha^4 \cos\alpha x - 2\sum_{m=1}^{\infty} Y_m'' \alpha^2 \cos\alpha x + \sum_{m=1}^{\infty} Y_m'''' \cos\alpha x = 0$$

or, $$\sum_{m=1}^{\infty} \left[Y_m'''' - 2\alpha^2 Y_m'' + \alpha^4 Y_m \right] \cos\alpha x = 0$$

or, $$Y_m'''' - 2\alpha^2 Y_m'' + \alpha^4 Y_m = 0 \qquad (2.4)$$

The solution of the above 4th order ordinary differential equation with constant coefficients [Eq. (2.4)] can normally be approximated as follows:

$$Y_m = A_m e^{r_1 y} + B_m y e^{r_2 y} + C_m e^{r_3 y} + D_m y e^{r_4 y} \qquad (2.5)$$

But the ordinary differential equation (2.4) has the complementary function of repeated roots. Thus $r_1 = r_2 = \alpha$, $r_3 = r_4 = -\alpha$ and the general solution of Eq. (2.4) can be written as

$$Y_m = \left(A_m + B_m y\right) e^{\alpha y} + \left(C_m + D_m y\right) e^{-\alpha y} \qquad (2.6)$$

where A_m, B_m, C_m and D_m are arbitrary constants.

Differentiating equation (3.6) following expressions are found

$$Y_m' = \left(A_m \alpha + B_m \alpha y + B_m\right) e^{\alpha y} + \left(-C_m \alpha - D_m \alpha y + D_m\right) e^{-\alpha y}$$

$$Y_m'' = \left(A_m \alpha^2 + B_m \alpha^2 y + 2B_m \alpha\right) e^{\alpha y} + \left(C_m \alpha^2 + D_m \alpha^2 y - 2D_m \alpha\right) e^{-\alpha y}$$

$$Y_m''' = \left(A_m \alpha^3 + B_m \alpha^3 y + 3B_m \alpha^3\right) e^{\alpha y} + \left(-C_m \alpha^3 - D_m \alpha^3 y + 3D_m \alpha^2\right) e^{-\alpha y}$$

$$Y_m'''' = \left(A_m \alpha^4 + B_m \alpha^4 y + 4B_m \alpha^3\right) e^{\alpha y} + \left(C_m \alpha^4 + D_m \alpha^4 y - 4D_m \alpha^3\right) e^{-\alpha y}$$

Now substituting the derivatives of ψ and Y_m in the expressions for displacement and stresses following expressions are found.

$$u_x(x,y)=\frac{\partial^2\psi}{\partial x\partial y}$$

$$=-\sum_{m=1}^{\infty}Y'_m\alpha\sin\alpha x$$

$$=-\sum_{m=1}^{\infty}\left[\left(A_m\alpha+B_m\alpha y+B_m\right)e^{\alpha y}+\left(-C_m\alpha-D_m\alpha y+D_m\right)e^{-\alpha y}\right]\alpha\sin\alpha x$$

$$=-\sum_{m=1}^{\infty}\left[A_m\alpha e^{\alpha y}+B_m(\alpha y+1)e^{\alpha y}-C_m\alpha e^{-\alpha y}-D_m(\alpha y-1)e^{-\alpha y}\right]\alpha\sin\alpha x \qquad (2.7a)$$

$$u_y(x,y)=-\frac{1}{(1+\mu)}\left[2\frac{\partial^2\psi}{\partial x^2}+(1-\mu)\frac{\partial^2\psi}{\partial y^2}\right]$$

$$=-\frac{1}{(1+\mu)}\left[2\left\{-\sum_{m=1}^{\infty}Y_m\alpha^2\cos\alpha x\right\}+(1-\mu)\left\{\sum_{m=1}^{\infty}Y''_m\cos\alpha x+6Ky\right\}\right]$$

$$=-\frac{1}{(1+\mu)}\left[\begin{array}{l}-2\sum_{m=1}^{\infty}\left\{\left(A_m+B_m y\right)e^{\alpha y}+\left(C_m+D_m y\right)e^{-\alpha y}\right\}\alpha^2\cos\alpha x+(1-\mu)\\ \sum_{m=1}^{\infty}\left\{\begin{array}{l}\left(A_m\alpha^2+B_m\alpha^2 y+2B_m\alpha\right)e^{\alpha y}+\\ \left(C_m\alpha^2+D_m\alpha^2 y-2D_m\alpha\right)e^{-\alpha y}\end{array}\right\}\cos\alpha x+6K(1-\mu)y\end{array}\right]$$

$$=\frac{-1}{(1+\mu)}\left[\sum_{m=1}^{\infty}\left\{\begin{array}{l}-A_m(1+\mu)\alpha^2e^{\alpha y}+\\ B_m\left(-\alpha y-\mu\alpha y-2\mu+2\right)\alpha e^{\alpha y}\\ -C_m(1+\mu)\alpha^2e^{-\alpha y}+\\ D_m\left(-\alpha y-\mu\alpha y+2\mu-2\right)\alpha e^{-\alpha y}\end{array}\right\}\cos\alpha x+6K(1-\mu)y\right] \qquad (2.7b)$$

$$\sigma_{xx}(x,y)=\frac{E}{(1+\mu)^2}\left[\frac{\partial^3\psi}{\partial x^2\partial y}-\mu\frac{\partial^3\psi}{\partial y^3}\right]$$

$$=\frac{E}{(1+\mu)^2}\left[\left\{-\sum_{m=1}^{\infty}Y'_m\alpha^2\cos\alpha x\right\}-\mu\left\{\sum_{m=1}^{\infty}Y'''_m\cos\alpha x+6K\right\}\right]$$

$$= \frac{-E}{(1+\mu)^2}\left[\begin{array}{l}\sum_{m=1}^{\infty}\left\{(A_m\alpha + B_m\alpha y + B_m)e^{\alpha y} + (-C_m\alpha - D_m\alpha y + D_m)e^{-\alpha y}\right\}\alpha^2\cos\alpha x \\ +\mu\sum_{m=1}^{\infty}\left\{\begin{array}{l}(A_m\alpha^3 + B_m\alpha^3 y + 3B_m\alpha^2)e^{\alpha y} + \\ (-C_m\alpha^3 - D_m\alpha^3 y + 3D_m\alpha^2)e^{-\alpha y}\end{array}\right\}\cos\alpha x + 6\mu K\end{array}\right]$$

$$= \frac{-E}{(1+\mu)^2}\left[\sum_{m=1}^{\infty}\left\{\begin{array}{l}A_m\alpha(1+\mu)e^{\alpha y} + B_m(\alpha y + \mu\alpha y + 3\mu + 1)e^{\alpha y} \\ -C_m\alpha(1+\mu)e^{-\alpha y} + D_m(-\alpha y - \mu\alpha y + 3\mu + 1)e^{-\alpha y}\end{array}\right\}\alpha^2\cos\alpha x + 6\mu K\right] \qquad (2.7c)$$

$$\sigma_{yy}(x,y) = \frac{-E}{(1+\mu)^2}\left[(2+\mu)\frac{\partial^3\psi}{\partial x^2\partial y} + \frac{\partial^3\psi}{\partial y^3}\right]$$

$$= \frac{-E}{(1+\mu)^2}\left[(2+\mu)\left\{-\sum_{m=1}^{\infty}Y_m'\alpha^2\cos\alpha x\right\} + \left\{\sum_{m=1}^{\infty}Y_m'''\cos\alpha x + 6K\right\}\right]$$

$$= \frac{-E}{(1+\mu)^2}\left[\begin{array}{l}-(2+\mu)\sum_{m=1}^{\infty}\left\{(A_m\alpha + B_m\alpha y + B_m)e^{\alpha y} + (-C_m\alpha - D_m\alpha y + D_m)e^{-\alpha y}\right\}\alpha^2\cos\alpha x \\ +\sum_{m=1}^{\infty}\left\{\begin{array}{l}(A_m\alpha^3 + B_m\alpha^3 y + 3B_m\alpha^2)e^{\alpha y} + \\ (-C_m\alpha^3 - D_m\alpha^3 y + 3D_m\alpha^2)e^{-\alpha y}\end{array}\right\}\cos\alpha x + 6K\end{array}\right]$$

$$= \frac{-E}{(1+\mu)^2}\left[\sum_{m=1}^{\infty}\left\{\begin{array}{l}A_m\alpha(-1-\mu)e^{\alpha y} + B_m(-\alpha y - \mu\alpha y - \mu + 1)e^{\alpha y} + \\ C_m\alpha(1+\mu)e^{-\alpha y} + D_m(\alpha y + \mu\alpha y - \mu + 1)e^{-\alpha y}\end{array}\right\}\alpha^2\cos\alpha x + 6K\right] \qquad (2.7d)$$

$$\sigma_{xy}(x,y) = \frac{-E}{(1+\mu)^2}\left[\frac{\partial^3\psi}{\partial x^3} - \mu\frac{\partial^3\psi}{\partial x\partial y^2}\right]$$

$$= \frac{-E}{(1+\mu)^2}\left[\sum_{m=1}^{\infty}Y_m\alpha^3\sin\alpha x - \mu\left\{-\sum_{m=1}^{\infty}Y_m''\alpha\sin\alpha x\right\}\right]$$

$$= \frac{-E}{(1+\mu)^2}[\sum_{m=1}^{\infty}\left\{(A_m + B_m y)e^{\alpha y} + (C_m + D_m y)e^{-\alpha y}\right\}\alpha^3\sin\alpha x +$$

$$\mu\sum_{m=1}^{\infty}\left\{\begin{array}{l}(A_m\alpha^2 + B_m\alpha^2 y + 2B_m\alpha)e^{\alpha y} + \\ (C_m\alpha^2 + D_m\alpha^2 y - 2D_m\alpha)e^{-\alpha y}\end{array}\right\}\alpha\sin\alpha x]$$

$$= \frac{-E}{(1+\mu)^2}\left[\sum_{m=1}^{\infty}\begin{Bmatrix} A_m(1+\mu)\alpha e^{\alpha y} + B_m(\alpha y + \mu\alpha y + 2\mu)e^{\alpha y} \\ + C_m(1+\mu)\alpha e^{-\alpha y} + D_m(\alpha y + \mu\alpha y - 2\mu)e^{-\alpha y} \end{Bmatrix}\alpha^2 \sin\alpha x\right] \qquad (2.7e)$$

Now, the reactions on the bottom boundary (y = 0) are acting over the two supports. It is considered that the supports are located at x=0 to 0.1L and x=0.9L to L respectively. The total length for reaction is 20 percent of beam length. Now the compressive load exerted at the mid-span on the edge $y = D$ of the beam may be considered as acting over at least some length of the beam, for instance x= 0.45L to 0.55L. As a result the intensity of reaction is half of the load intensity. Therefore, the reactions over the beam at the supports can be taken as Fourier series in the following manner:

$\sigma_{yy}(x, D) = \sigma_0 = I_0 + \sum_{m=1}^{\infty} I_m \cos\alpha x$ For x= 0.45L to 0.55L

Here

$$I_0 = \frac{1}{L}\left[\int_{9L/20}^{11L/20} \sigma_0 dx\right] = \frac{\sigma_0}{10} \qquad (2.8a)$$

$$I_m = \frac{2}{L}\left[\int_{9L/20}^{11L/20} \sigma_0 \cos\alpha x dx\right]$$

$$= \frac{2\sigma_0}{\alpha L}\left\{\sin\left(\frac{11\alpha L}{20}\right) - \sin\left(\frac{9\alpha L}{20}\right)\right\}$$

$$= \frac{2\sigma_0}{m\pi}\left\{\sin\left(\frac{11m\pi}{20}\right) - \sin\left(\frac{9m\pi}{20}\right)\right\} \qquad (2.8b)$$

The reaction load at the support on the edge $y = 0$ can also be given by a Fourier series as follows

$\sigma_{yy}(x,0) = \sigma_0 / 2 = E_0 + \sum_{m=1}^{\infty} E_m \cos\alpha x$ For x=0 to 0.1L and 0.9L to L

Here

$$E_0 = \frac{1}{L}\left[\int_0^{L/10} \sigma_0 / 2dx + \int_{9L/10}^{L} \sigma_0 / 2dx\right] = \frac{\sigma_0}{10} \tag{2.9a}$$

$$\begin{aligned} E_m &= \frac{2}{L}\left[\int_0^{L/10} \frac{\sigma_0}{2}\cos\alpha x dx + \int_{9L/10}^{L} \frac{\sigma_0}{2}\cos\alpha x dx\right] \\ &= \frac{\sigma_0}{\alpha L}\left\{\sin\left(\frac{\alpha L}{10}\right) - 0 + \sin(\alpha L) - \sin\left(\frac{9\alpha L}{10}\right)\right\} \\ &= \frac{\sigma_0}{m\pi}\left\{\sin\left(\frac{m\pi}{10}\right) + \sin(m\pi) - \sin\left(\frac{9m\pi}{10}\right)\right\} \end{aligned}$$

The loading considerations of equations (2.8a) and (2.9a) are to satisfy the boundary conditions at the bottom and top boundaries of the beam. Using boundary condition $\sigma_{xy}(x,0) = 0$ at the edge of $y = 0$, it is found that

$$\frac{-E}{(1+\mu)^2}\left[\sum_{m=1}^{\infty}(A_m + C_m)\alpha^3 \sin\alpha x + \mu\sum_{m=1}^{\infty}\left\{\begin{matrix}\left(A_m\alpha^2 + 2B_m\alpha\right)+ \\ \left(C_m\alpha^2 - 2D_m\alpha\right)\end{matrix}\right\}\alpha\sin\alpha x\right] = 0$$

or, $$\frac{-E}{(1+\mu)^2}\left[(A_m + C_m)\alpha^3 + \mu\left\{\left(A_m\alpha^2 + 2B_m\alpha\right) + \left(C_m\alpha^2 - 2D_m\alpha\right)\right\}\alpha\right] = 0$$

or, $$\frac{-E}{(1+\mu)^2}\left[(1+\mu)\alpha^3 A_m + 2B_m\mu\alpha^2 + (1+\mu)\alpha^3 C_m - 2\mu\alpha^2 D_m\right] = 0$$

or, $$\frac{-E\alpha^2}{(1+\mu)^2}\left[(1+\mu)\alpha A_m + 2\mu B_m + (1+\mu)\alpha C_m - 2\mu D_m\right] = 0 \tag{2 .12a}$$

Using boundary condition $\sigma_{xy}(x,D) = 0$ at the edge of $y = D$

$$\frac{-E}{(1+\mu)^2}\left[\begin{matrix}\sum_{m=1}^{\infty}\left\{\left(A_m + B_m D\right)e^{\alpha D} + \left(C_m + D_m D\right)e^{-\alpha D}\right\}\alpha^3 \sin\alpha x + \\ \mu\sum_{m=1}^{\infty}\left\{\begin{matrix}\left(A_m\alpha^2 + B_m\alpha^2 D + 2B_m\alpha\right)e^{\alpha D} + \\ \left(C_m\alpha^2 + D_m\alpha^2 D - 2D_m\alpha\right)e^{-\alpha D}\end{matrix}\right\}\alpha\sin\alpha x\end{matrix}\right] = 0$$

$$\text{or, } \frac{-E}{(1+\mu)^2}\begin{bmatrix}\{(A_m+B_mD)e^{\alpha D}+(C_m+D_mD)e^{-\alpha D}\}\alpha^3+\\ \mu\{(A_m\alpha^2+B_m\alpha^2D+2B_m\alpha)e^{\alpha D}+\\ (C_m\alpha^2+D_m\alpha^2D-2D_m\alpha)e^{-\alpha D}\}\alpha\end{bmatrix}=0$$

$$\text{or, } \frac{-E\alpha^2}{(1+\mu)^2}\begin{bmatrix}A_m(1+\mu)\alpha e^{\alpha D}+B_m(\alpha D+\mu\alpha D+2\mu)e^{\alpha D}+\\ C_m(1+\mu)\alpha e^{-\alpha D}+D_m(\alpha D+\mu\alpha D-2\mu)e^{-\alpha D}\end{bmatrix}=0 \qquad (2.12a)$$

Using boundary condition $\sigma_{yy}(x,0)=\sigma_0/2$ at the edge of $y=0$

$$\frac{-E}{(1+\mu)^2}\begin{bmatrix}-(2+\mu)\sum_{m=1}^{\infty}\{(A_m\alpha+B_m)+(-C_m\alpha+D_m)\}\alpha^2\cos\alpha x\\ +\sum_{m=1}^{\infty}\{(A_m\alpha^3+3B_m\alpha^2)+\\ (-C_m\alpha^3+3D_m\alpha^2)\}\cos\alpha x+6K\end{bmatrix}=\sum_{m=1}^{\infty}E_m\cos\alpha x+E_o \qquad (2.13a)$$

Therefore,

$$\frac{E\alpha^2}{(1+\mu)^2}\begin{bmatrix}(2+\mu)\{(A_m\alpha+B_m)+(-C_m\alpha+D_m)\}\\ -(A_m\alpha+3B_m)-(-C_m\alpha+3D_m)\end{bmatrix}=E_m$$

$$\text{or, } \frac{E\alpha^2}{(1+\mu)^2}[A_m(1+\mu)\alpha+B_m(-1+\mu)-C_m(1+\mu)\alpha+D_m(-1+\mu)]=E_m \qquad (2.13b)$$

Using boundary condition $\sigma_{yy}(x,D)=\sigma_0$ at the edge of $y=D$

$$\frac{-E}{(1+\mu)^2}\begin{bmatrix}-(2+\mu)\sum_{m=1}^{\infty}\{(A_m\alpha+B_m\alpha D+B_m)e^{\alpha D}+\\ (-C_m\alpha-D_m\alpha D+D_m)e^{-\alpha D}\}\alpha^2\cos\alpha x\\ +\sum_{m=1}^{\infty}\{(A_m\alpha^3+B_m\alpha^3D+3B_m\alpha^2)e^{\alpha D}+\\ (-C_m\alpha^3-D_m\alpha^3D+3D_m\alpha^2)e^{-\alpha D}\}\cos\alpha x+6K\end{bmatrix}=\sum_{m=1}^{\infty}I_m\cos\alpha x+I_o \qquad (2.14a)$$

$$\frac{E}{(1+\mu)^2}\begin{bmatrix}(2+\mu)\{(A_m\alpha+B_m\alpha D+B_m)e^{\alpha D}+(-C_m\alpha-D_m\alpha D+D_m)e^{-\alpha D}\}\alpha^2\\ -\{(A_m\alpha^3+B_m\alpha^3D+3B_m\alpha^2)e^{\alpha D}+(-C_m\alpha^3-D_m\alpha^3D+3D_m\alpha^2)e^{-\alpha D}\}\end{bmatrix}=I_m$$

$$\text{or, } \frac{E\alpha^2}{(1+\mu)^2}\begin{bmatrix} A_m(1+\mu)\alpha e^{\alpha D} + B_m(\mu\alpha D + \alpha D + \mu - 1)e^{\alpha D} - \\ C_m(1+\mu)\alpha e^{-\alpha D} - D_m(\mu\alpha D + \alpha D - \mu + 1)e^{-\alpha D} \end{bmatrix} = I_m \tag{2.14b}$$

and using Eq. (2.9a) and Eq. (2.13a) the arbitrary constant K can be obtained as follows:

$$\frac{-E}{(1+\mu)^2}6K = E_0 = \frac{\sigma_0}{10}$$

$$\text{or, } K = \frac{-\sigma_0(1+\mu)^2}{60E} \tag{2.15}$$

The simultaneous equations (2.12a), (2.12b), (2.13b) and (2.14b) can be realized in a simplified matrix form for the solution of unknown terms like A_m, B_m, C_m and D_m as follows:

$$\begin{bmatrix} DD_1 & DD_2 & DD_3 & DD_4 \\ FF_1 & FF_2 & FF_3 & FF_4 \\ HH_1 & HH_2 & HH_3 & HH_4 \\ KK_1 & KK_2 & KK_3 & KK_4 \end{bmatrix}\begin{bmatrix} A_m \\ B_m \\ C_m \\ D_m \end{bmatrix} = \begin{bmatrix} 0 \\ 0 \\ E_m \\ I_m \end{bmatrix} \tag{2.16}$$

where

$$DD_1 = Z_{11}(1+\mu)\alpha$$
$$DD_2 = 2\mu Z_{11}$$
$$DD_3 = Z_{11}(1+\mu)\alpha$$
$$DD_4 = -2\mu Z_{11}$$

$$FF_1 = Z_{11}(1+\mu)\alpha e^{\alpha D}$$
$$FF_2 = Z_{11}\{(1+\mu)\alpha D + 2\mu\}e^{\alpha D}$$
$$FF_3 = Z_{11}(1+\mu)\alpha e^{-\alpha D}$$
$$FF_4 = Z_{11}\{(1+\mu)\alpha D - 2\mu\}e^{-\alpha D}$$
$$HH_1 = -Z_{11}(1+\mu)\alpha$$
$$HH_2 = -Z_{11}(-1+\mu)$$
$$HH_3 = Z_{11}(1+\mu)\alpha$$
$$HH_4 = -Z_{11}(-1+\mu)$$

$$KK_1 = -Z_{11}(1+\mu)\alpha e^{\alpha D}$$
$$KK_2 = -Z_{11}\{(1+\mu)\alpha D + \mu - 1\}e^{\alpha D}$$

$$KK_3 = Z_{11}(1+\mu)\alpha e^{-\alpha D}$$
$$KK_4 = Z_{11}\{(1+\mu)\alpha D - \mu + 1\}e^{-\alpha D}$$

$$Z_{11} = \frac{-E\alpha^2}{(1+\mu)^2}$$

Therefore, stress and displacement components at various points of the beam can be obtained using equations of (2.7).

CHAPTER 3
ANALYSIS OF THE RESULTS

The analytical solutions of displacement and stress components are obtained for various aspect ratios (L/D) of the beam. The material of the beam is mild steel whose modulus of elasticity is E=209 X 10^9 and poison's ratio μ=0.3. The result of a guided isotropic beam having aspect ratio two and three and the uniform loading parameter σ_0 = 40 N/mm is presented in sequence of axial displacement (u_x), lateral displacement (u_y), bending stress (σ_{xx}), normal stress (σ_{yy}) and shearing stress (σ_{xy}).

3.1 Solution of Displacement Components

Axial displacements (u_x) are found to be zero at the mid section of span and at the lateral guided boundaries. Zero value of u_x at the guided ends verifies the boundary condition of those edges of the beam. Axial displacements distribution is found skew-symmetric about the mid-span of the beam. The values of u_x for sections $0<x/L< 0.5$ are negative at the lower portion and positive at upper portion of the beam. The maximum magnitudes of $u_x/L= \pm 0.000158$ are observed on bottom fibre at the sections of x/L = 0.1 and x/L = 0.9 respectively.

For aspect ratio L/D=3 the shape of axial displacement curve remains unchanged but magnitude of displacement is increased

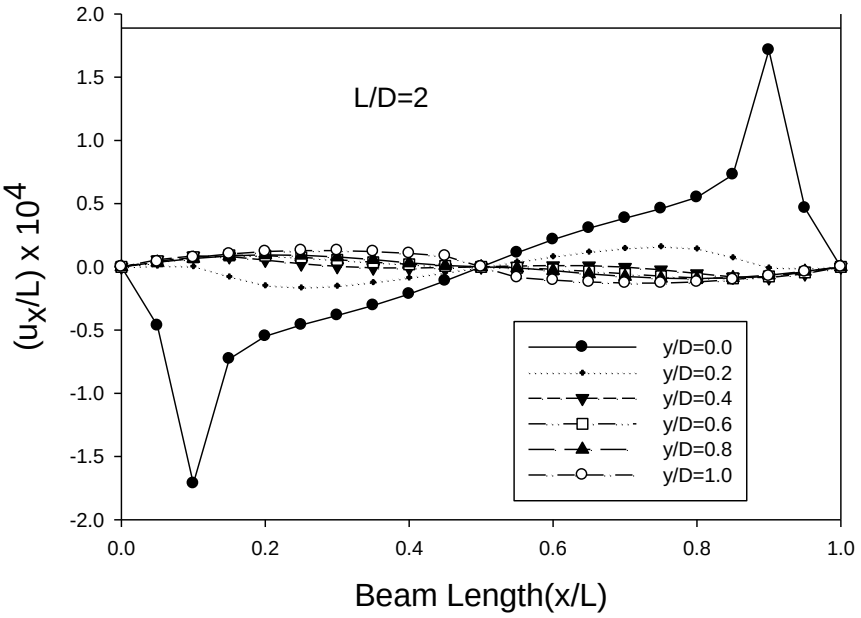

Fig 3.1: Axial displacement at longitudinal sections for L/D=2

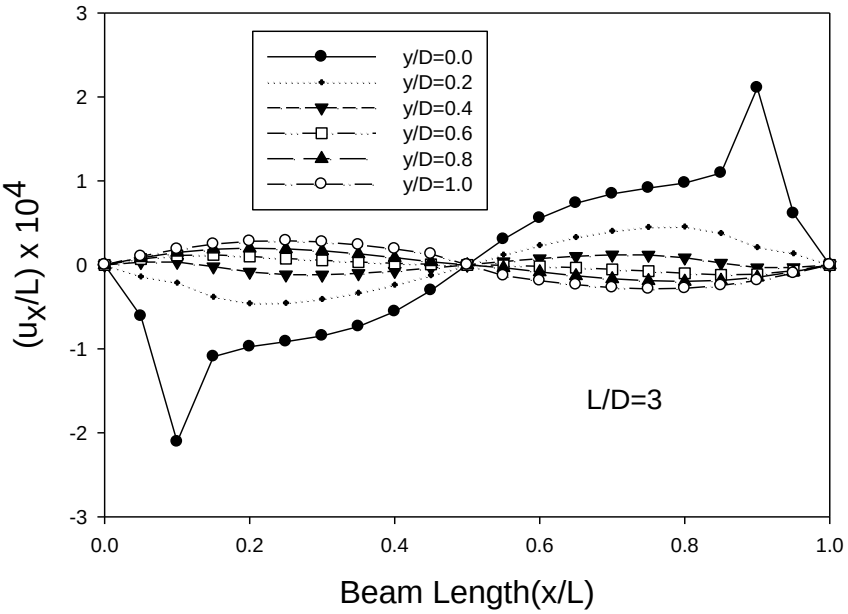

Fig 3.2: Axial displacement at longitudinal sections for L/D=3

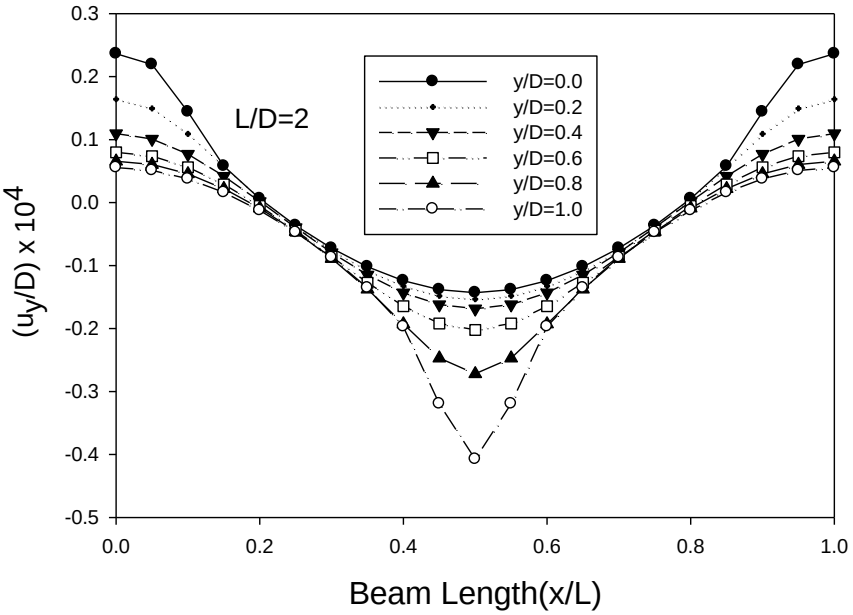

Fig 3.3: Lateral displacement at longitudinal sections for L/D=2

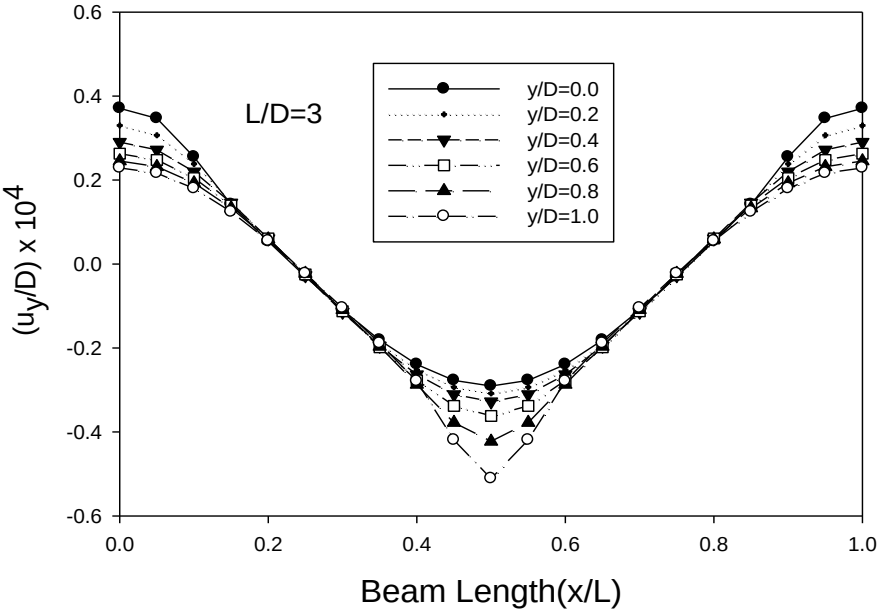

Fig 3.4: Lateral displacement at longitudinal sections for L/D=3

Lateral displacements (u_y) are found to take positive value near the two guided lateral ends and negative in the region $0.25<x/L< 0.75$ for L/D=2 and for L/D=3 it is negative in the region $0.2<x/L<0.8$, on account of loading at top edge and balanced by two bottom corner support . There is no restriction on the lateral displacement other than the loading and reaction to bring the beam in equilibrium state. The u_y results are in confirmation to the physical condition of the beam. As a result the beam is being pushed up at the corners and forced down at the mid-span region. The normalized values of positive and negative maximum lateral displacements are $u_y/D=0.000250$ and $u_y/D= - 0.000426$ respectively for L/D=2. For L/D=3 it is $u_y/D= -0.00045$ and $u_y/D= 0.00029$.The maximum magnitude is observed on the topmost fibre at the mid-span.

Along beam depth both for L/D=2 and L/D=3 maximum axial displacement occurs at x/L=0.1.

Maximum lateral displacement occurs at x/L=0.5 for both L/D=2 and L/D=3 .

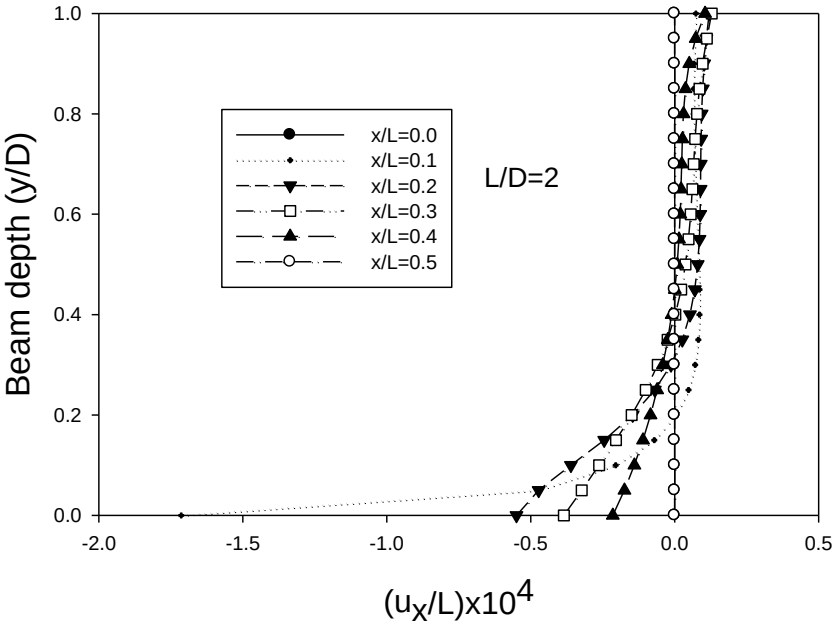

Fig 3.5: Axial displacement at transverse section for L/D=2

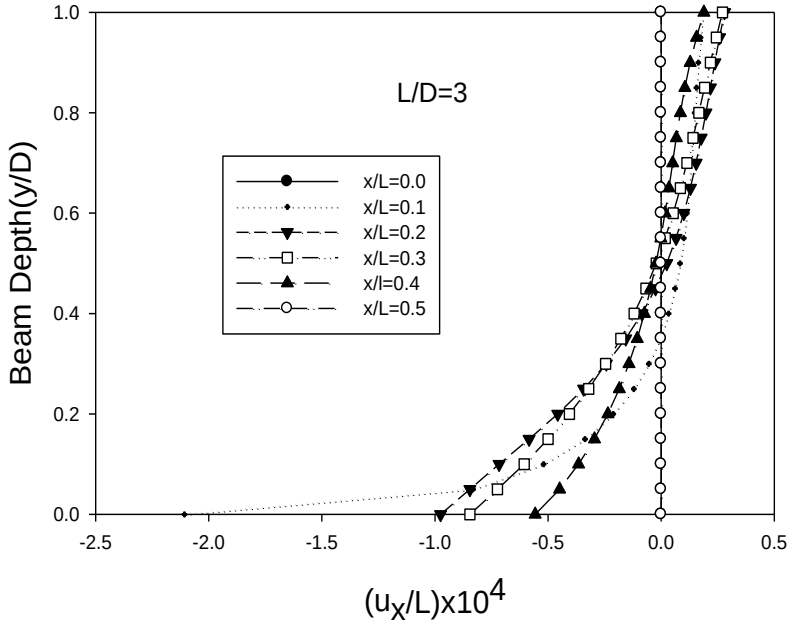

Fig 3.6: Axial displacement at transverse section for L/D=3

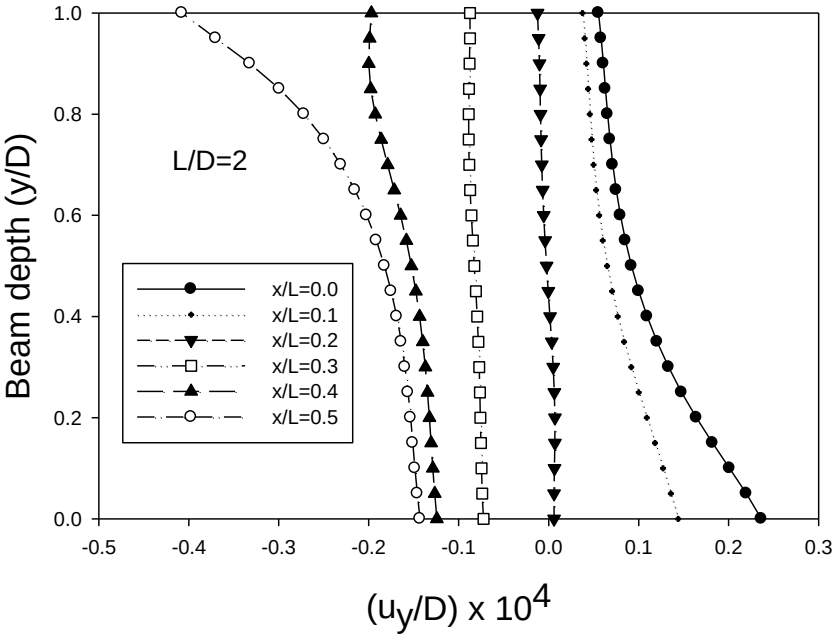

Fig 3.7 Lateral displacement for transverse section for L/D=2

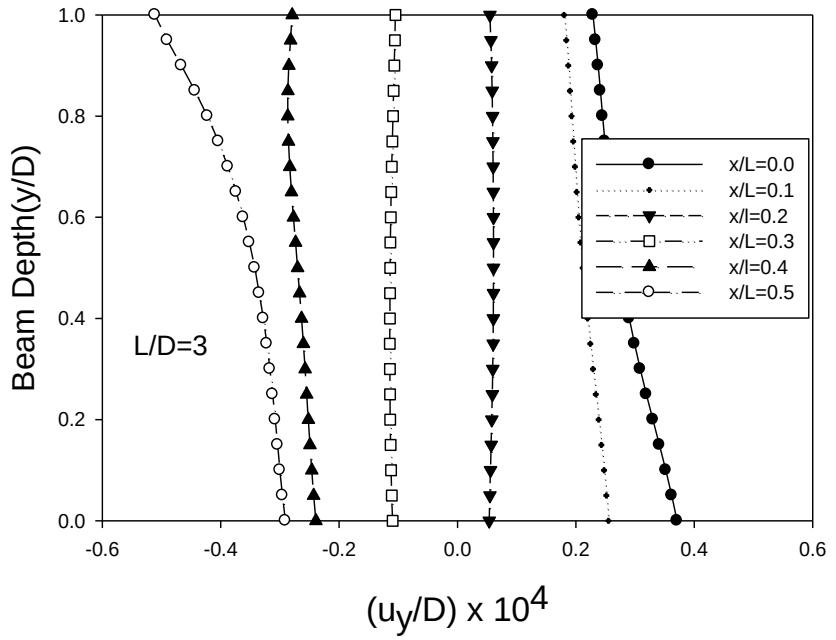

Fig 3.8 Lateral displacement for transverse section for L/D=3

3.2 Solution of Stresses

Bending stress distribution is observed non-linear over the whole span. The stress (σ_{xx}) maximizes at the mid-span top fibre of the beam where the point type load is acting. The next locations of bending stress concentration are the two bottom corners and the bottom fibre at mid-span of the beam. The maximum magnitude of normalized bending stress on the top fibre at mid-span is a 1.19.

Lateral stress (σ_{yy}) concentrations are observed at the topmost fibre of mid-span section and Bottom two corners. It is understandable that each reaction is half of the load and the normalized value of the lateral stress varies from zero to about unity at the topmost layer in the loaded region and it is almost half at the bottom layer of the support region, which confirms the physical condition of the problem

All four edges and mid-span section of the guided simply supported beam are found free from shearing stress. The distribution of shearing stress (σ_{xy}) for point loading is anti-symmetric in two sides about the mid-span of the beam like distributed load. The maximum concentration of shearing stress is observed near the bottom corners at the supports and the point of shear stress concentration is at the top edge where the termination of loading takes place. The normalised maximum magnitude of shear stress is ±0.2 for L/D=2 and +- 0.24 for L/D=3 on y/D=0.8.

Shear stress distribution at transverse section is nearly parabolic. Along beam depth maximum shear occurs at x/L=0.2 and normalised value of this shear stress is -0.18.Shear stress is zero at x/L=0.4

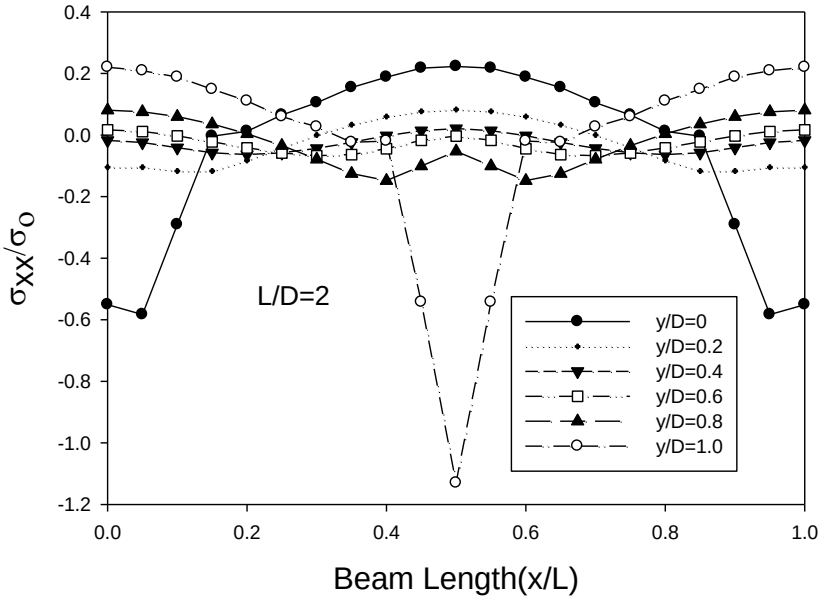

Fig 3.9: Bending stress distribution at longitudinal section for L/D=2

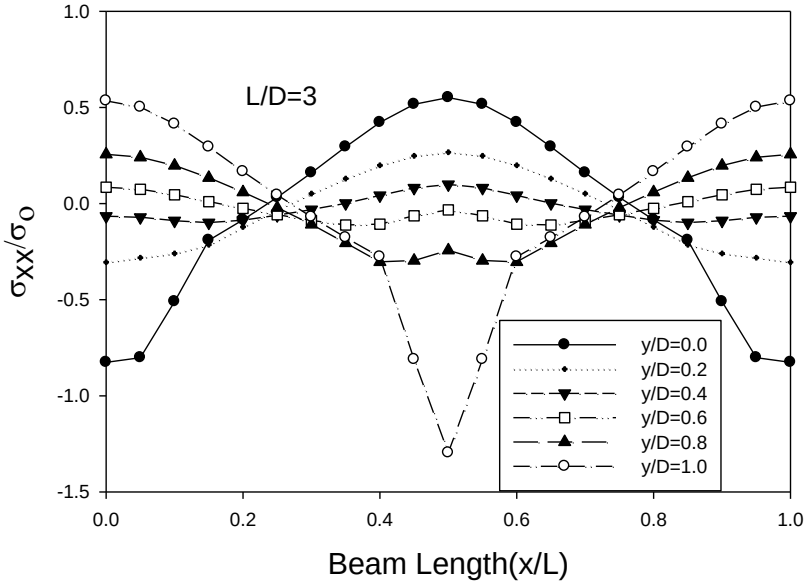

Fig 3.10 Bending stress distribution at longitudinal section for L/D=3

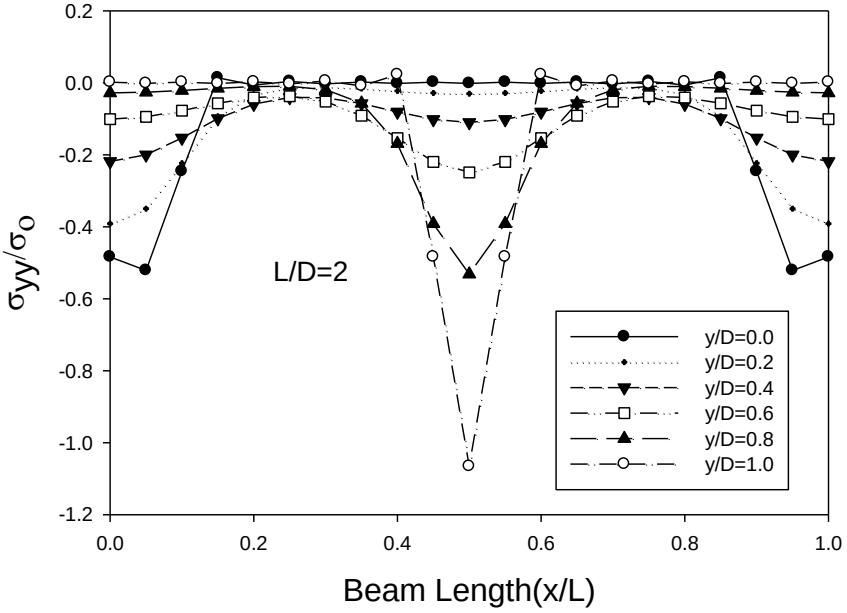

Fig 3.11: Lateral stress distribution at longitudinal section for L/D=2

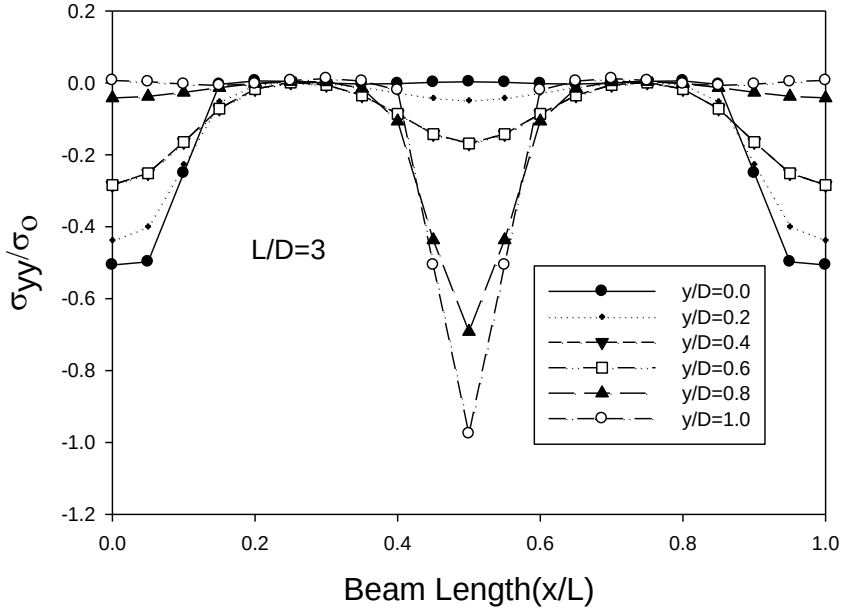

Fig 3.12: Lateral stress distribution at longitudinal section for L/D=3

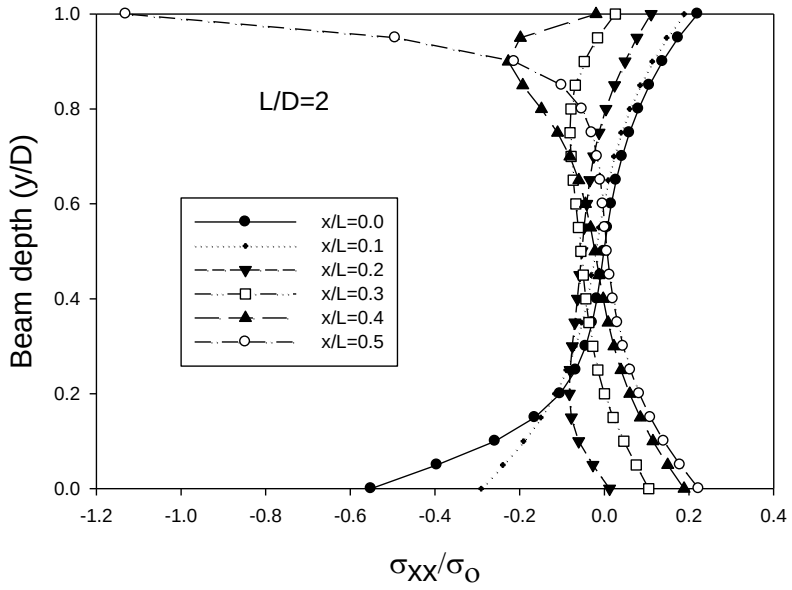

Fig 3.13: Bending stress distribution at transverse section for L/D=2

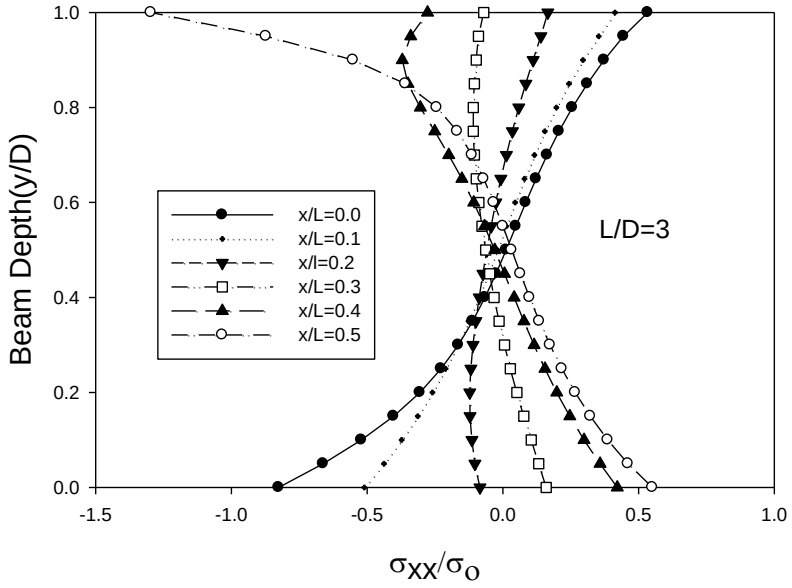

Fig 3.14: Bending stress distribution at transverse section for L/D=3

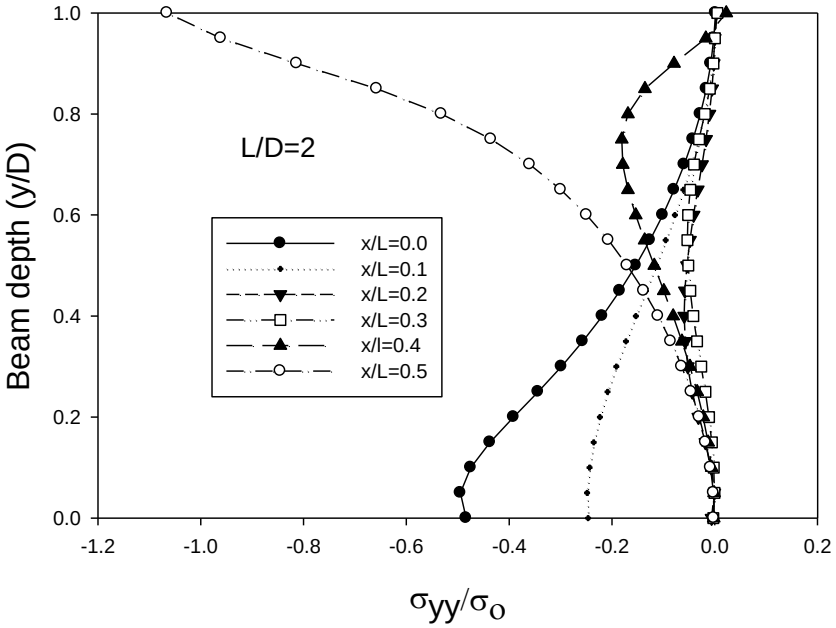

Fig 3.15: Lateral stress distribution at transverse section for L/D=2

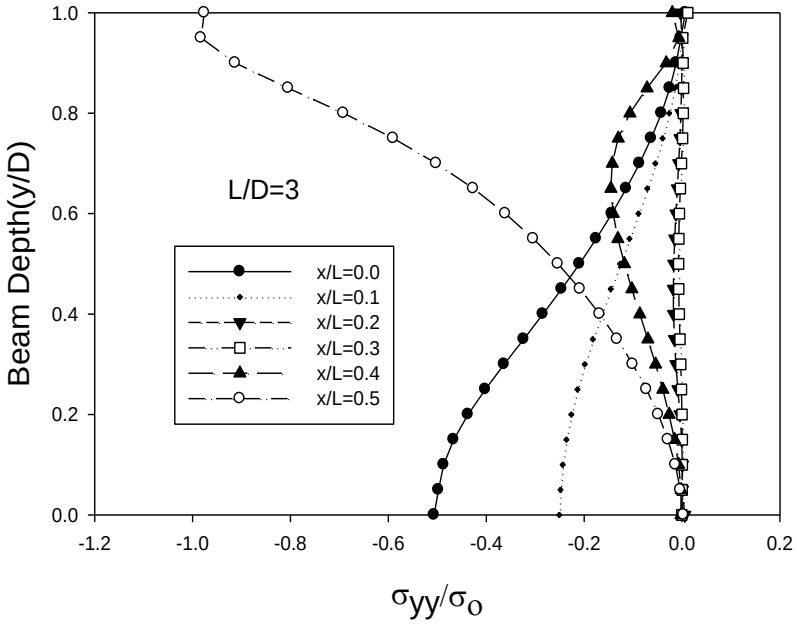

Fig 3.16: Lateral stress distribution at transverse section for L/D=3

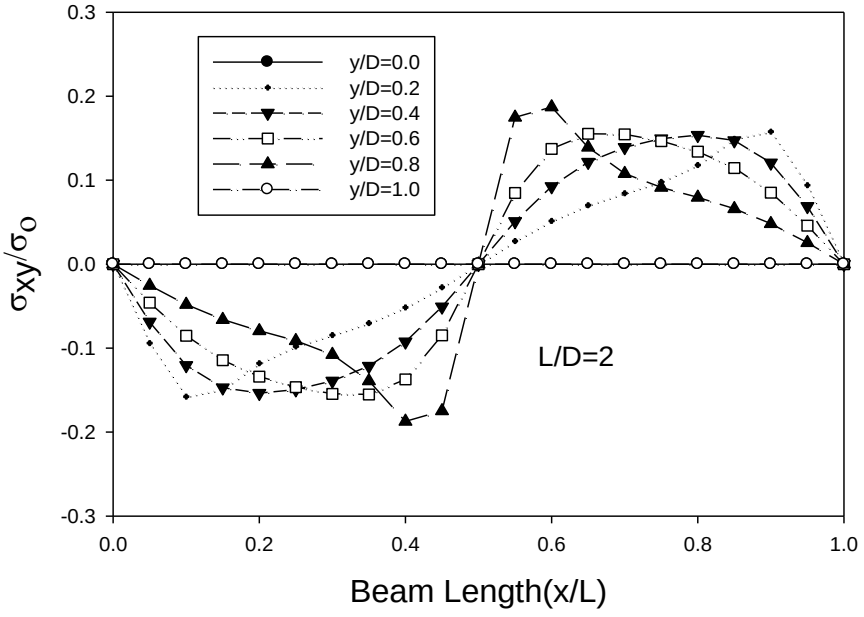

Fig 3.17: Shear stress distribution at longitudinal section for L/D=2

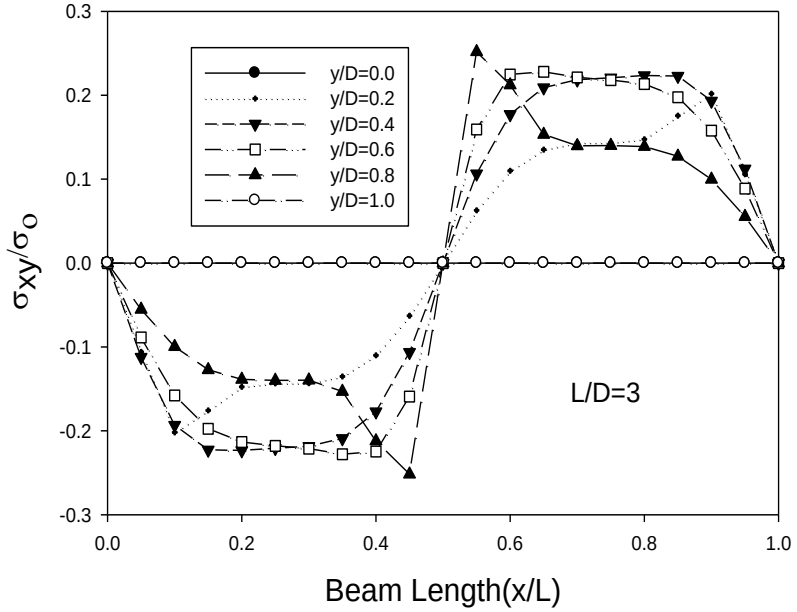

Fig 3.18: Shear stress distribution at longitudinal section for L/D=3

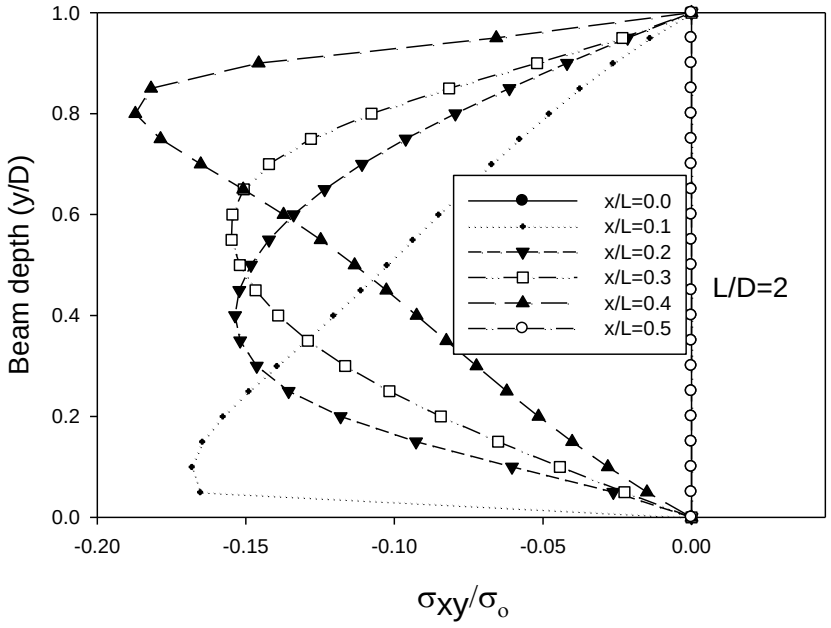

Fig 3.19 Shear stress distribution at transverse section for L/D=2

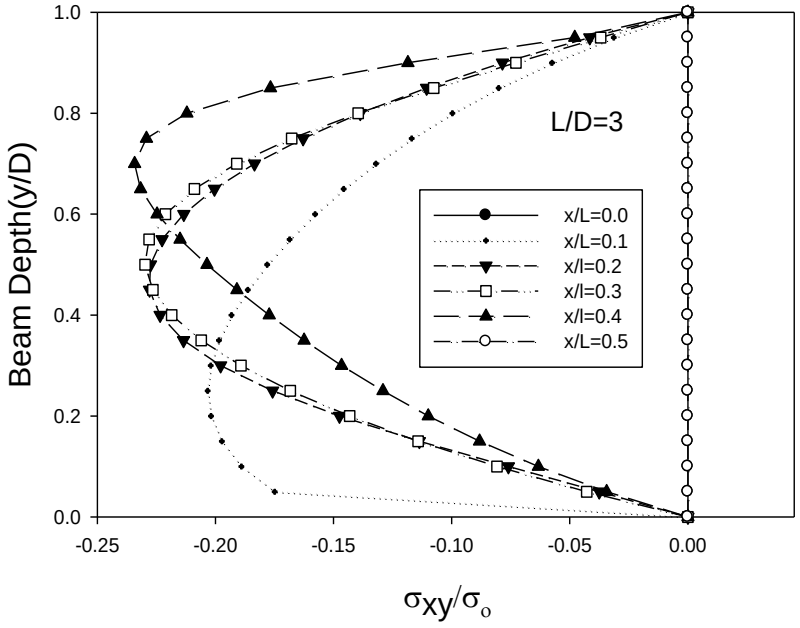

Fig 3.20: Shear stress distribution at transverse section for L/D=3

3.3 Comparison of displacement

As the aspect ratio increases the magnitude of both axial and lateral displacement increases. The sharp changes in the curve become gradually smoother for higher aspect ratio such as 6, 8, 10, and 12.

Along beam depth as the aspect ratio increases the curvature of the curves decreases and they become straighter. The magnitude of the displacement also increases.

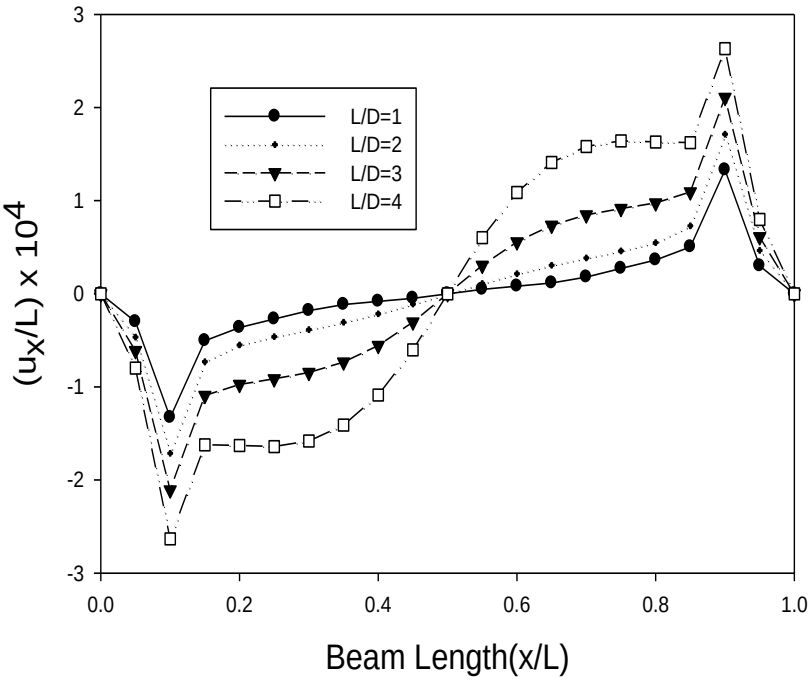

Fig 3.21Comparison of axial displacement for L/D=1, 2, 3, 4 at y/D=0.0

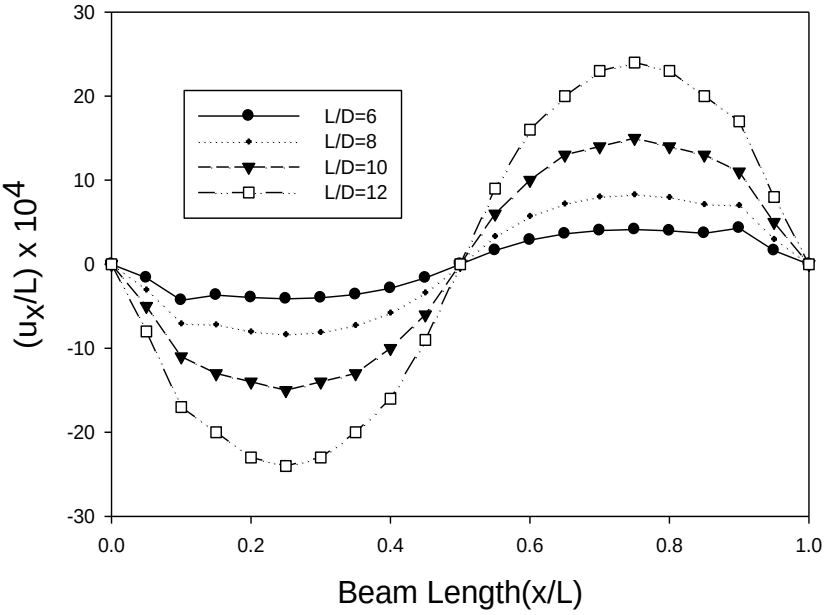

Fig 3.22 Comparison of axial displacement for L/D=6, 8, 10, 12 at y/D=0.0

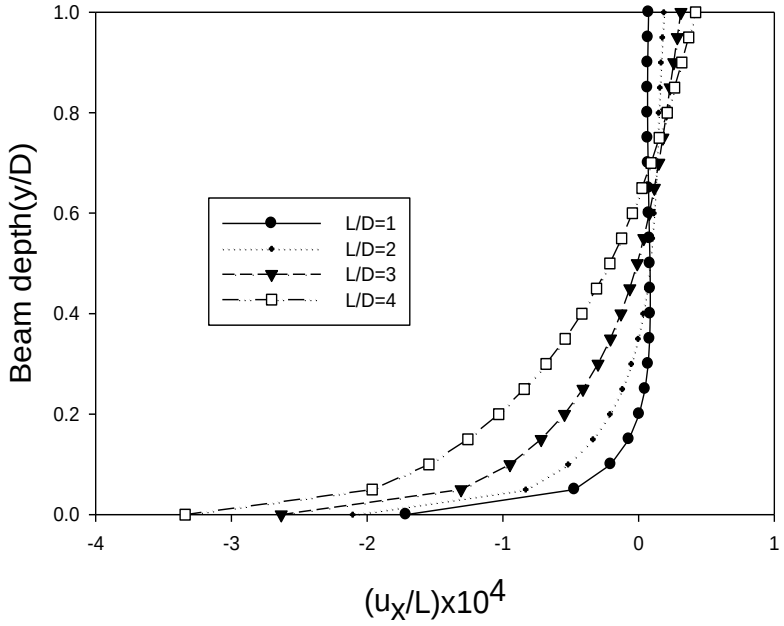

Fig 3.23 Comparison of axial displacement along transverse section for L/D=1, 2, 3, 4 at x/L=0.1

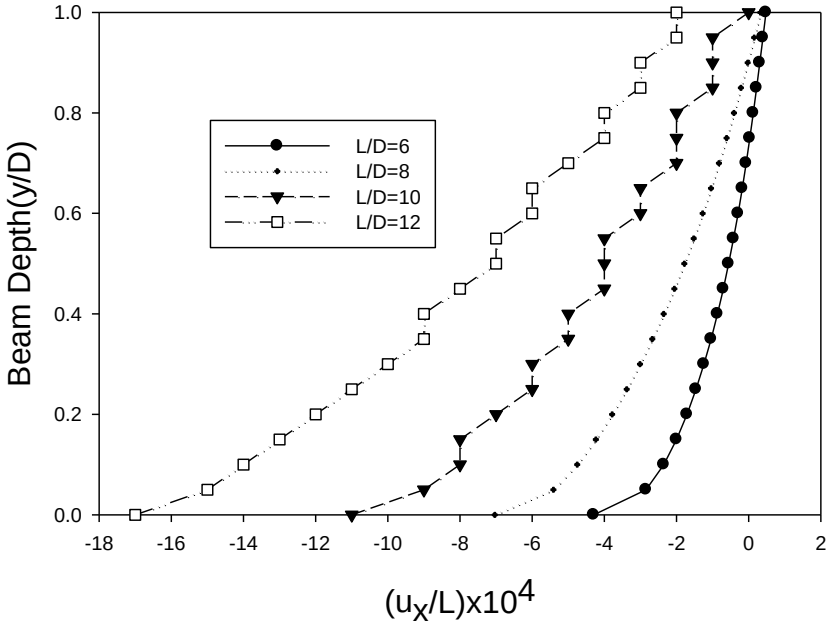

Fig 3.24 Comparison of axial displacement along transverse section for L/D=6, 8, 10, 12 at x/L=0.1

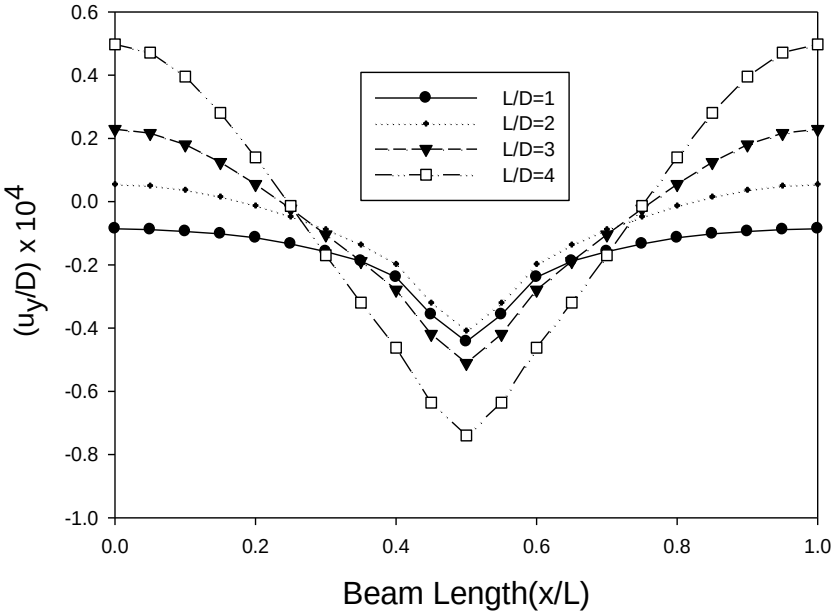

Fig 3.25 Comparison of lateral displacement along longitudinal section for L/D=1, 2, 3, 4 at y/D=1.0

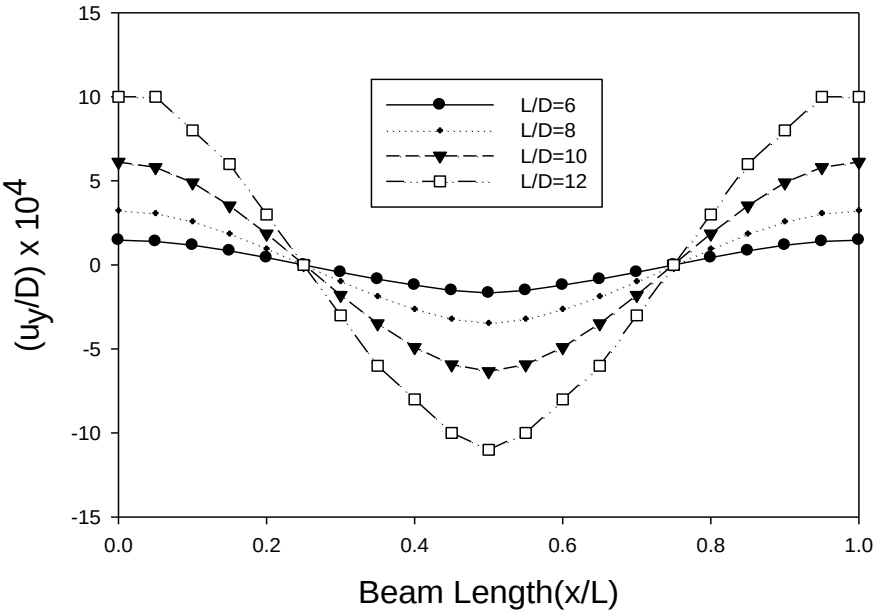

Fig 3.26 Comparison of lateral displacement along longitudinal section for L/D=6, 8, 10, 12 at y/D=1.0

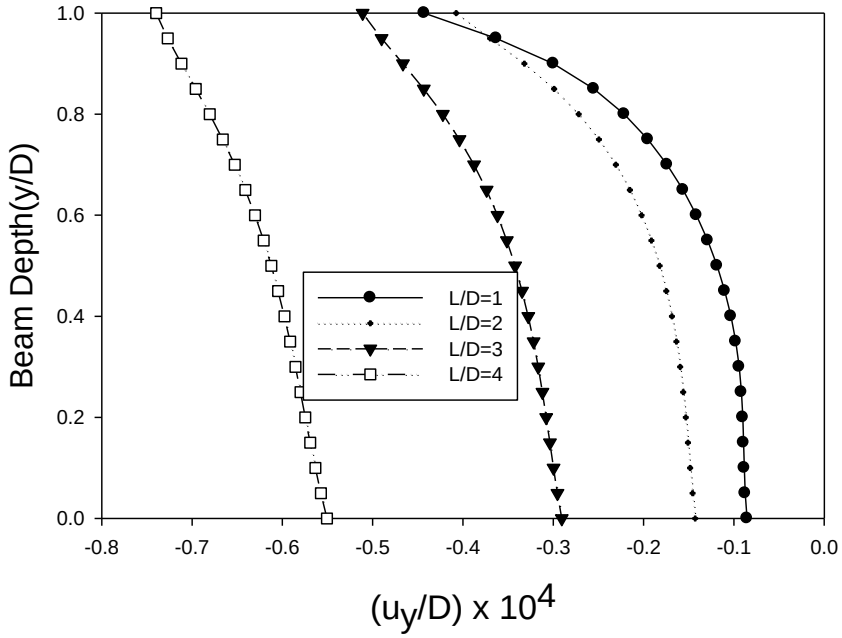

Fig 3.27 Comparison of lateral displacement along transverse section for L/D=1, 2, 3, 4 at x/L=0.5

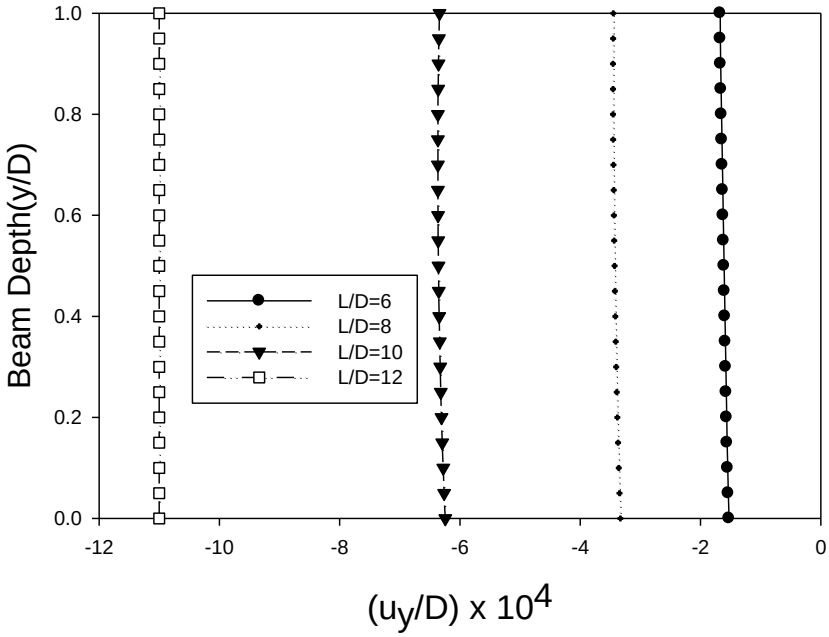

Fig 3.28 Comparison of lateral displacement along transverse section for L/D=6, 8, 10, 12 at x/L=0.5

3.4 Comparison of stresses

As the aspect ratio increases the bending stress also increases. For L/D=4 the magnitude of bending stress is -1.8 at x/L=0.5.Bending stress is zero at x/L=0.25 and x/L=0.8.With the increase in aspect ratio the curve becomes smoother and magnitude increases in both positive and negative direction.

The lateral stress remains almost same with the increase in aspect ratio. Stress concentration occurs at section x/L=0.5. At other section its value is almost zero.

Along beam depth at section y/D=0.5 bending stress is zero. With the increase in aspect ratio bending stress increases along beam depth. The curve becomes straighter as the aspect ratio increases.

Shear stress increases as the aspect ratio increases along beam length. For L/D=4 it varies from -0.3 to +0.3.For L/D =12 its value varies from -0.8 to +0.8.

As the aspect ratio increases shear stress assumes more and more standard parabolic shape along beam depth.

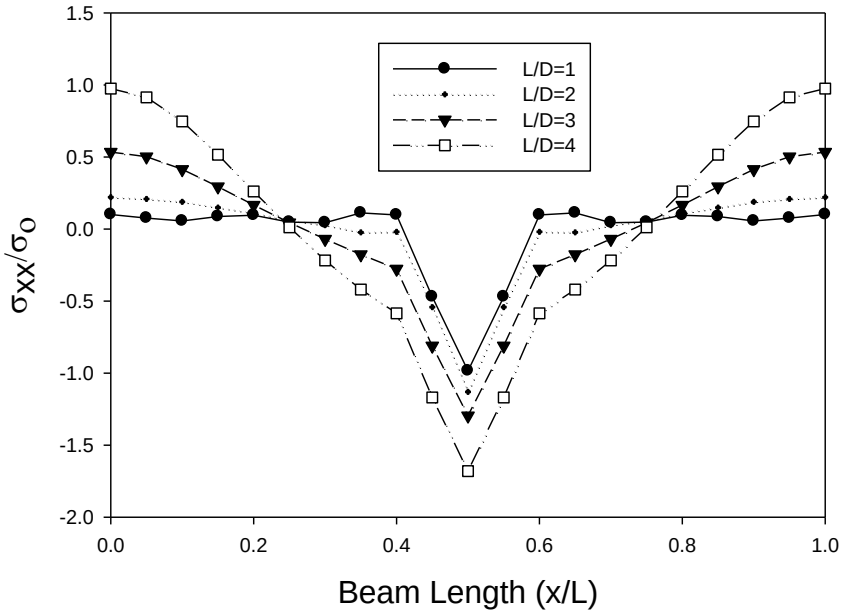

Fig 3.29 Comparison of bending stress along longitudinal section for L/D=1, 2, 3, 4 at y/D=1.0

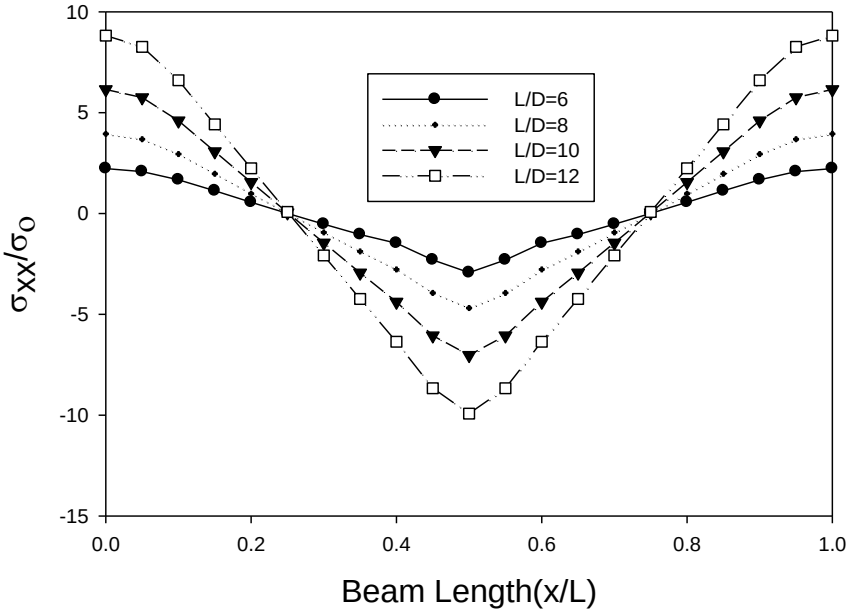

Fig 3.30 Comparison of bending stress along longitudinal section for L/D=6, 8, 10, 12 at y/D=1.0

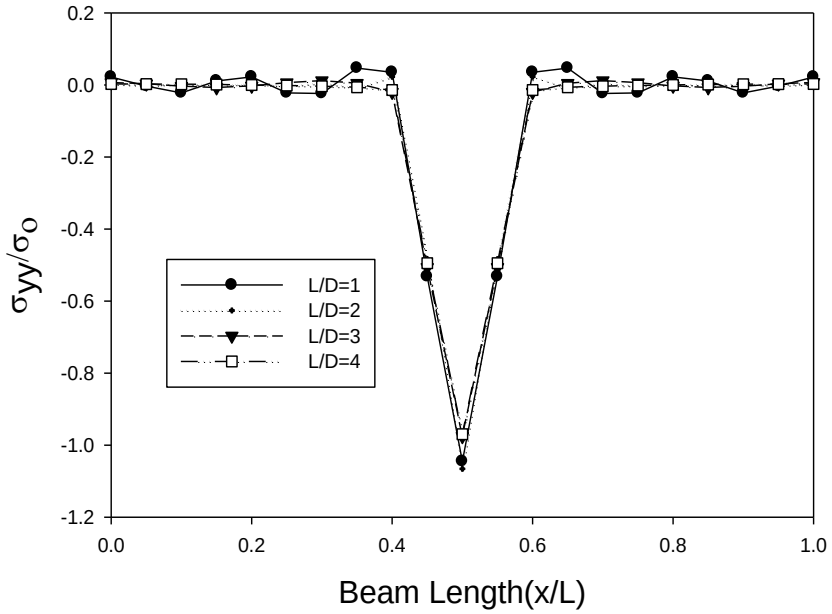

Fig 3.31 Comparison of lateral stress along longitudinal section for L/D=1, 2, 3, 4 at y/D=1.0

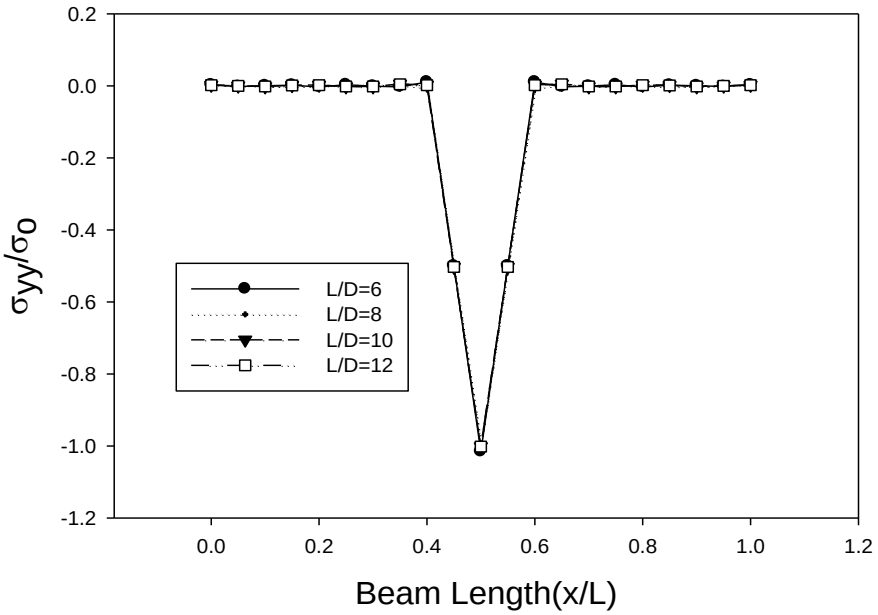

Fig 3.32 Comparison of lateral stress along longitudinal section for L/D=6, 8, 10, 12 At y/D=1.0

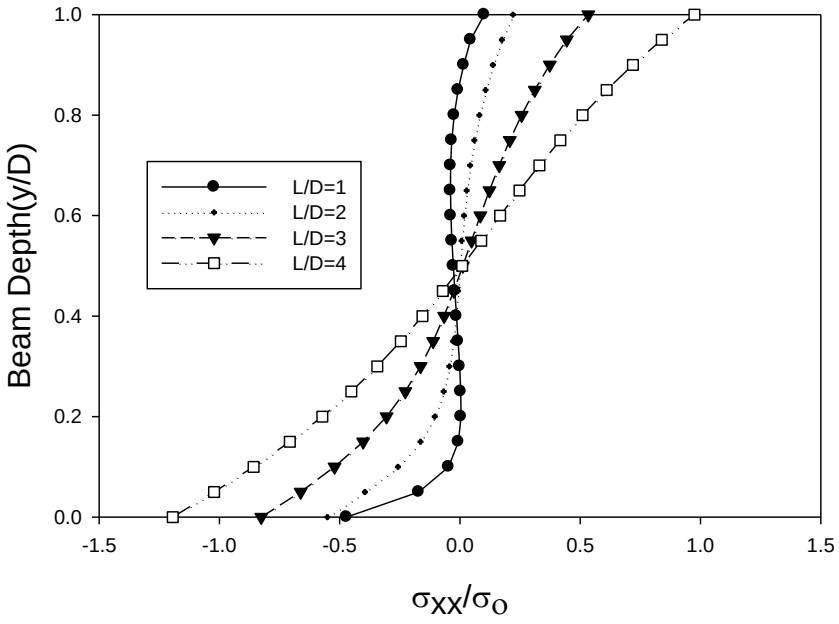

Fig 3.33 Comparison of bending stress along transverse section for L/D=1, 2, 3, 4 at x/L=0.5

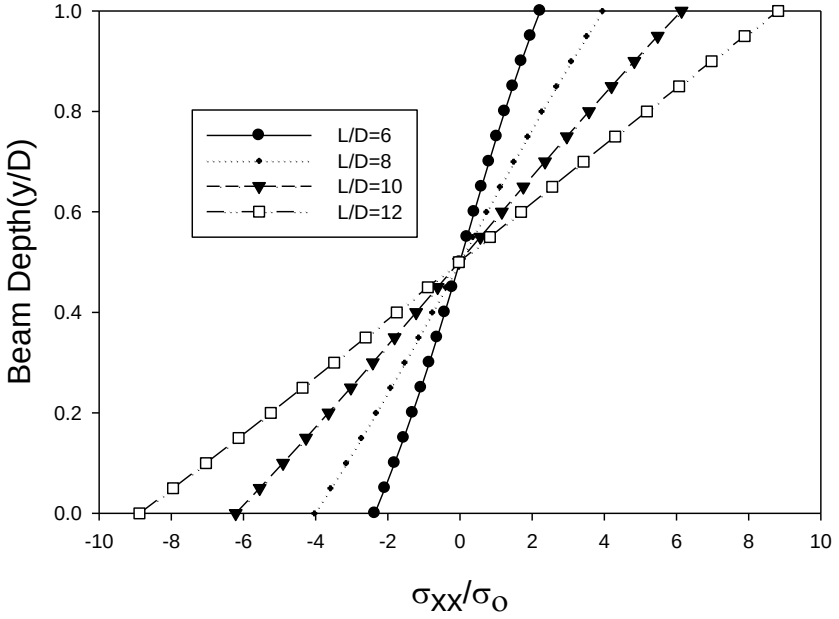

Fig 3.34 Comparison of bending stress along transverse section for L/D=6, 8, 10, 12 At x/L=0.5

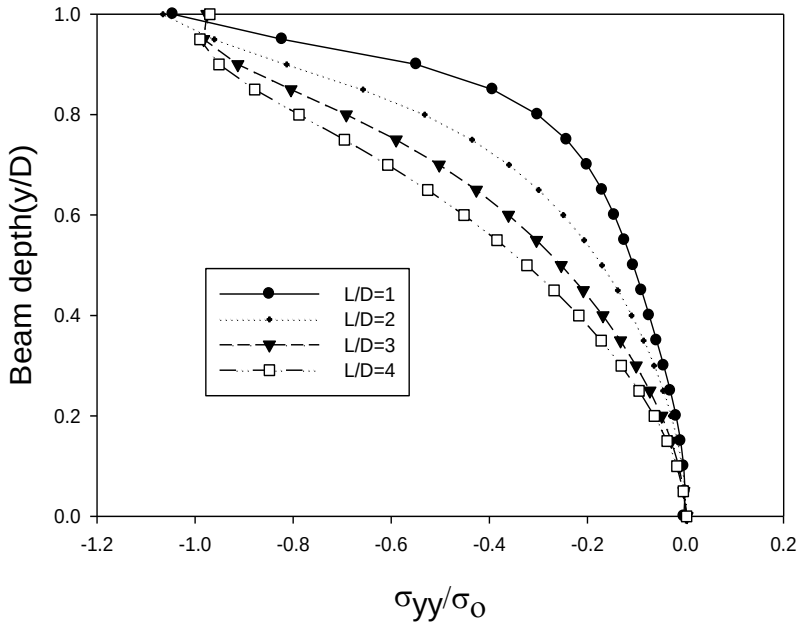

Fig 3.35Comparison of lateral stress along transverse section for L/D=1, 2, 3, 4 At x/L=0.5

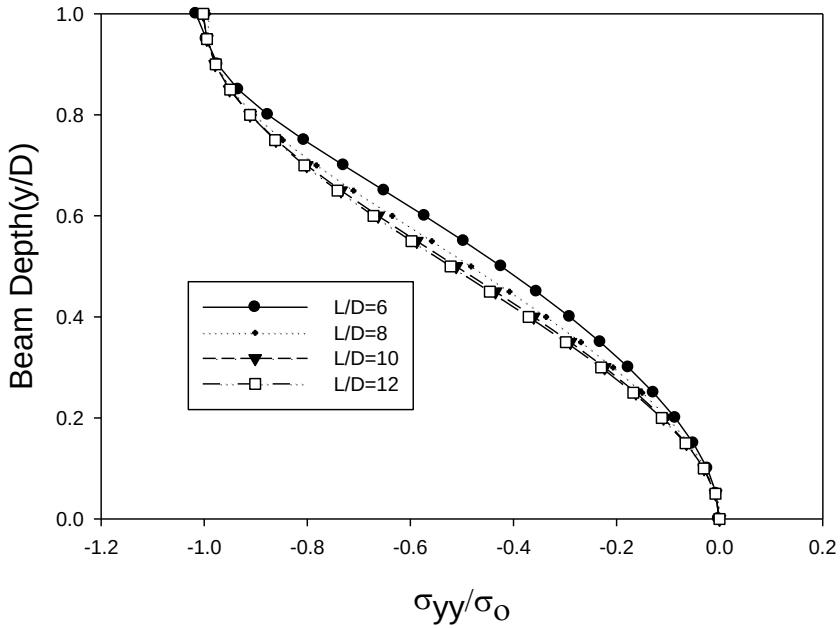

Fig 3.36 Comparison of lateral stress along transverse section for L/D=6, 8, 10, 12 At x/L=0.5

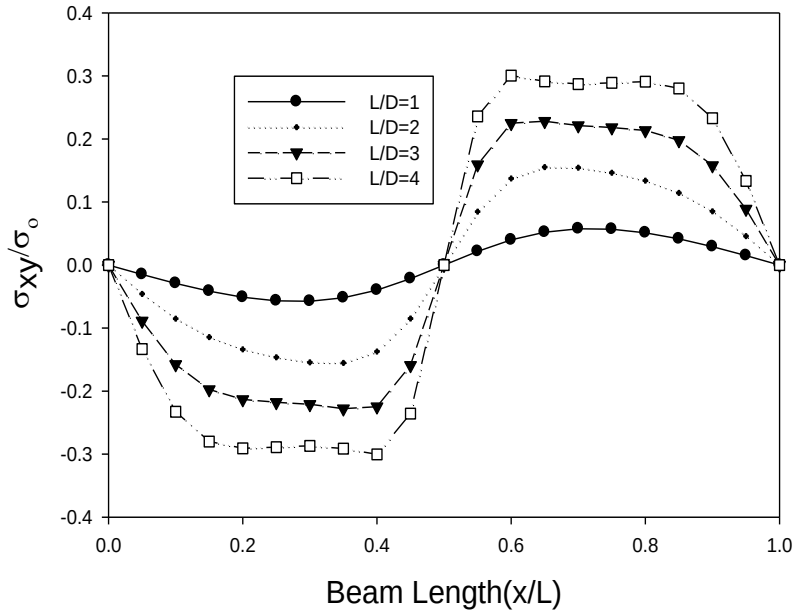

Fig 3.37 Comparison of shear stress along longitudinal section for L/D=1, 2, 3, 4
At y/D=0.8

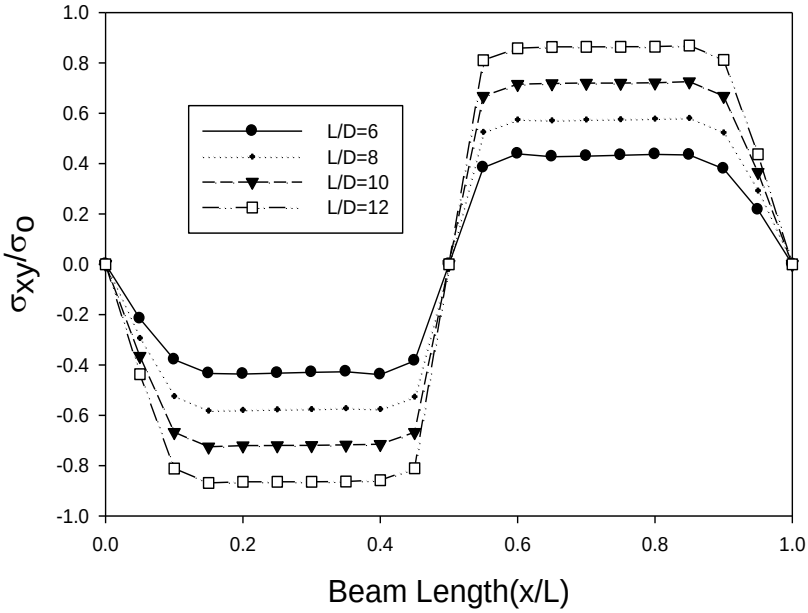

Fig 3.38 Comparison of shear stress along longitudinal section for L/D=6, 8, 10, 12
At y/D=0.8

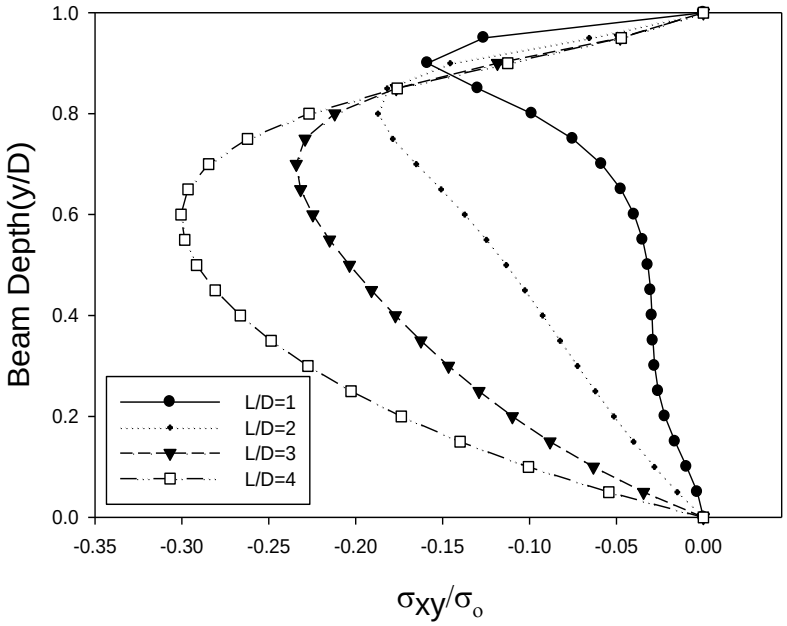

Fig 3.39 Comparison of shear stress along transverse section for L/D= 1, 2, 3, 4 At x/L=0.4

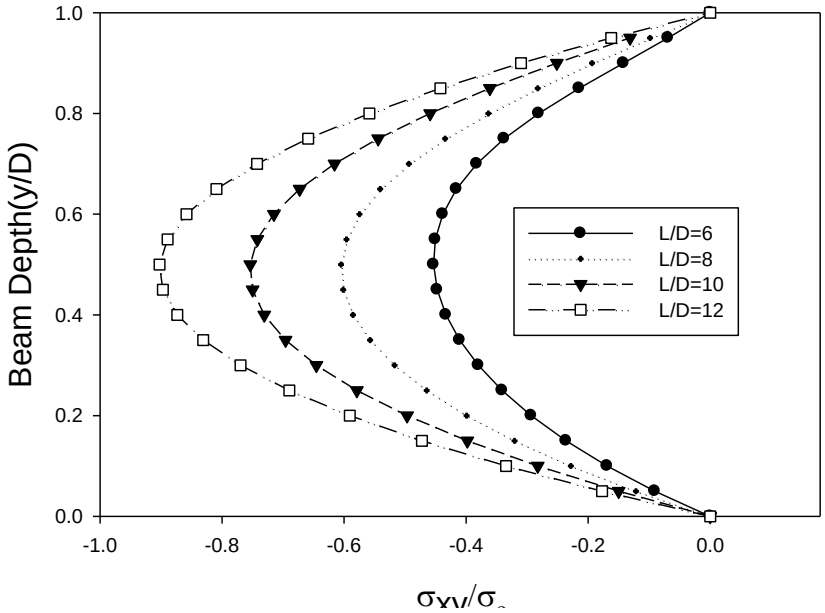

Fig 3.40 Comparison of shear stress along transverse section for L/D= 6, 8, 10, 12 At x/L=0.4

3.5 Summary

Analytical solution using displacement potential approach for the elastic fields of a guided deep beam of isotropic material under three point bending is explored satisfying all the physical conditions of the beam appropriately. The solution of anisotropic beam for the aspect ratio two and three is observed for symmetric loading.The solutions indicate that thedisplacement potential approach can address three point bending of isotropic materials effectively. Displacement and stress components are of the similar maximum values also. The stress concentration is investigated and found to be at the near location of point load.

CONCLUSIONS

The central objective of this research is to develop the analytical solutions for guided simply supported beams. The speciality of the guided ends is the mixed mode of boundary conditions. Basically, the guided ends provide the freedom of lateral displacement but not the axial one. At this scenario the necessity of imposing boundary restraints is essential. But it is not practicable to use the classical Bernoulli-Euler beam theory for the solution of guided beam. Because it cannot handle mixed mode of boundary conditions. Displacement potential formulation can handle mixed mode of boundary condition appropriately and we have found the solution of the beam.

It is observed from the solution of the beam that

1. Axial displacement is maximum at bottom fibre i.e y/D=0.0 .As the aspect ratio increases axial displacement also increases.
2. Lateral displacement is maximum at top fibre i.e y/D=1.0 . As the aspect ratio increases lateral displacement also increases. So if failure occurs it will occur at midsection of the beam i.e where deflection is maximum.
3. Maximum stress concentration occurs at midsection of the beam .So in terms of stress midsection is more vulnerable to failure for a simply supported beam.

RECOMMENDATIONS

These results of a simply supported beam can be further verified by commercial software like ANSYS.

The computer program used in this research is written in FORTRAN language. If this program can be written in MATLAB then it will be more user friendly. So if anybody who wants to carry on this research in future it is recommended to convert the program into MATLAB for better efficiency.

Experiment can be performed and the results of the experiment can be compared to the analytical solution of the simply supported beam.

REFERENCES

1. Airy, G.B., British Association for the Advancement of Science Report, 1862.

2. Timoshenko, S.P. and Goodier, J. N., Theory of Elasticity, -3rd Ed., McGraw Hill Book Co., New York, 1970.

3. Borg, S. F., Fundamentals of Engineering Elasticity, World Scientific, Singapore, 2nd ed., 1990.

4. Rankine, Applied Mechanics, 14th ed., pp. 344, 1895.

5. Grashof, Elastizitt Festigkcit, 2nd ed., 1878.

6. Levy, M., Compt. Rend, Vol. 126, pp. 1235, 1898.

7. Scewald, F., Abhandl, Aerodynamic Inst. Tech. Hochschule, Achen, vol.7, pp. 11, 1927.

8. Ribiere, M. C., Sur divers cas de la flexon des primes rectangles, thesis, Bordeux, 1889.

9. Filon, L.N.G., Phil, trans., Series A, vol. 201, pp. 63,1903.

10. Bleich, F., Bauingenieur, vol. 4, pp. 255, 1923.

11. Beyer, K., Die Statik in Esienbetonban, 2d ed, pp723, 1934.

12. Ribiere, Compt, Rend. Vol. 132. pp. 315, 1901.

13. Flamant, Compt. Rend, Paris, vol. 114. pp. 1465, 1892.

14. Stokes, G.G., Mathematical and Physical Papers, vol. 5, p.238, 1935.

15. Conway, H. D., Chow, L., and Morgan, G.W., "Analysis of deep beams," Journal of Applied Mechanics, Trans ASME 18(2), 163–172, 1951.

16. Chow, L., Conway, H. D., and Winter, G., "Stresses in Deep Beams", Trans ASCE, Paper No. 2557, 1952.

17. Conway, H. D., and Ithaca, N. Y., "Some problems of orthotropic plane stress," Journal of Applied Mechanics, Trans ASME, 52, 72–76, 1953.

18. Chapel, R. E., and Smith, H. W., "Finite-Difference solutions for plane stresses," AIAA Journal 6, 1156–1157, 1968.

19. Parker, D. F., "The role of Saint-Venant's Solutions in rod and beam theories," Journal of Applied Mechanics, Trans ASME 46, 861–866, 1979.

20. Horgan, C. O., and Knowels, J. K., "Recent developments concerning Saint-Venant's Principle," Advances in Applied Mechanics, 23, 179–269, 1983.

21. Horgan, C. O., and Simmonds, J. G., " Saint-Venant End Effects in Composite Structures," Composite Engineering, Vol 4, No 3, 279–286, 1994.

22. John Wiley & Sons Inc, Handbook of Experimental Stress Analysis, New York, 1950.

23. Frocht, M.M., Photoelasticity, John Wiley & Sons Inc, New York, vol.2, 1948.

24. Uddin, M. W., "Finite Difference Solution of Two-dimensional Elastic Problems with mixed Boundary Conditions", M. Sc. Thesis, Carleton University, Canada, 1966.

25. Durelli, A. J., and Ranganayakamma, B., "Parametric solution of stresses in beams," Journal of Engineering Mechanics 115(2), 401–414, 1989.

26. Rehfield, L. W. and Murthy, L. N., "Toward a new engineering theory of bending: Fundamentals", AIAA Journal, vol. 20. pp.693-699, 1982.

27. Murty A. V. K., "Towards a consistent beam theory", AIAA Journal, vol. 22. pp.811-816, 1984.

28. Suzuki S., Stress analysis of short beams, AIAA Journal, vol.24. pp.1396-1398, 1986.

29. Hardy S. J. and Pipelzadeh M. K., "Static analysis of short beams, Journal of strain Analysis", vol. 26, No. 1, pp.15-29, 1991.

30. Ahmed, S. R., Idris, A. B. M., and Uddin, M. W., "Numerical solution of both ends fixed deep beams," Computers & Structures 61(1), 21–29, 1996.

31. Ahmed, S. R., Khan, M. R., Islam, K. M. S., and Uddin, M. W., "Investigation of stresses at the fixed end of deep cantilever beams," Computers &Structures 69, 329–338, 1998.

32. Ahmed S.R., Idris A.B.M. and Uddin M.W., "An alternative method for numerical Solution of mixed boundary value elastic problems". Journal of Wave-Material Interaction, vol.14, No.1-2, pp.12-25, 1999.

33. Ahmed, S. R., Hossain, M. Z. and Uddin, M.W., "A general mathematical formulation for finite-difference solution of mixed-boundary-value problems of anisotropic materials," Computers & Structures, 83, 35–51, 2005.

34. Akanda, M. A. S., Ahmed, S. R. and Uddin, M. W., “Stress analysis of gear teeth using displacement potential function and finite differences,” International Journal for Numerical Methods in Engineering, 53, 1629–1640, 2002.

35. Ahmed, S. R., Nath, S. K. D., and Uddin, M.W., “Optimum shapes of tire treads for avoiding lateral slippage between tires and roads,” International Journal for Numerical Methods in Engineering, 64, 729–750, 2005.

36. Nath, S. K. D., Ahmed, S. R., and Afsar, A. M., “Displacement potential solution of short stiffened flat composite bars under axial loadings,” International Journal of Applied Mechanics and Engineering 11(3), 557–575, 2006.

37. Nath, S. K. D., Afsar, A. M., and Ahmed, S. R., “Displacement potential approach to solution of stiffened orthotropic composite panels under uniaxial tensile load,” Journal of Aerospace Engineering, Part G, IMechE, 221(5), 896–881, 2007.

38. Mukhopadhyay, M., “Mechanics of Composite Materials and Structures,” Universities Press, Hydrabad, pp46, 2004.

39. Jones, R. M., “Mechanics of Composite Materials,” Taylor Francis, Philadelphia, 1999.

40. Kaw, A. K., “Mechanics of Composite Materials,” CRC Press LLC, 1997.